Petrology, geochemistry and petrogenesis of the dykes from the Zhob Ophiolite, Pakistan

Abstract

The highly deformed Zhob ophiolite comprises the Ali Khanzai, Naweoba, and Omzha blocks. Each of these blocks contains both felsic and mafic dyke swarms. The felsic dykes occur as patches and pods in gabbroic bodies of crustal sections while mafic dykes crosscut the mantle peridotite of these blocks. Felsic dykes are plagiogranite and are composed of quartz, plagioclase and accessory ferromagnesian minerals whereas mafic dykes are basaltic in composition and contain largely plagioclase, clinopyroxene, and hornblende with minor quartz grains. Major, trace and rare earth elements have been analyzed in the felsic and mafic to assess the tectonomagmatic setting of the Zhob ophiolite. The felsic dykes are calc-alkaline oceanic plagiogranites while mafic dykes are tholeiitic in composition. Chondrite normalized patterns for the felsic dykes are characterized by low values of the REEs and positive Eu anomalies which indicate that they were formed by partial melting of basic rocks under hydrous conditions. The mafic dykes show very slight Nb depletion and enrichment in large ion lithophile elements (LILE) over high field strength elements (HFSE) which suggest that mafic dyke swarms are derived from an undepleted mantle source. Oceanic rocks with such characteristics are generally thought to have formed by processes involving a subduction zone component in the source region by fluids released from the subducting slab. These features suggest a subduction related setting which indicates an island arc, back arc or supra-subduction zone affinity for the formation of both felsic and mafic dykes of the Zhob ophiolite.

Keywords: Mafic and felsic dykes, plagiogranite, supra-subduction zone, Zhob ophiolite

1. Introduction

Ophiolites are fragments of oceanic lithosphere that have been obducted tectonically along continental margins during orogenic processes. An intact ophiolite has almost a complete stratigraphy from mantle peridotite to crustal rocks (Robertson, 2002). Partial melting of peridotites produces mafic melt which forms the oceanic crust while the partial melting of the mafic rocks of oceanic crust under hydrous conditions produces minor felsic rocks known as plagiogranites (Klein and Langmuir, 1987; Arndt et al., 2009; Korenaga, 2013). Fractional crystallization of basaltic magma and partial melting of the mafic rocks have been proposed

for the formation of the felsic and basaltic dyke swarms, respectively (Beccaluva et al., 1999; France et al., 2010; Wanless et al., 2010; Brophy and Pu, 2012).

The Bela-Zhob Valley-Waziristan ophiolitic belt extends from south to north in Pakistan and demarcates the western boundary of the Indian plate with the Afghan block of Eurasian plate (Fig. 1a; Gansser, 1979). The Zhob Valley contains three ophiolites namely Khanozai, Muslim Bagh and Zhob Ophiolites (Fig. 1b). Studies suggest that the felsic and mafic dyke swarms of Waziristan and Muslim Bagh ophiolites (north and south of Zhob ophiolite, respectively) formed in a subduction-related setting (island arc, back arc basin and supra-subduction zone setting) (Khan et al., 2001; Kakar et al., 2014). The Zhob ophiolite contains three detached blocks: the Naweoba, Omzha and Ali Khanzai blocks (Fig. 1c, d, e), which are highly tectonised. It is therefore challenging to distinguish the different rock types in these deformed blocks. All blocks of Zhob Ophiolite contain ultramafic gabbros and volcanic rocks (Naeem et al., 2021, 2022; Khan et al., 2020a, b). These rocks were first reported as intrusive bodies by Jones (1961), however, prior to this study little petrographic data and no geochemistry was available on these rocks. In this study, we report the first detailed fieldwork, petrography and the first major and trace element geochemistry of the felsic and mafic dyke swarms from the Zhob ophiolite in Pakistan to determine the geologic and tectonic setting of the Zhob ophiolite and the origin of the dykes.

2. Geological Setting

The Zhob ophiolitic blocks are part of the Waziristan-Muslim Bagh ophiolites of Neo-Tethyan origin that represent the suture zone between the Indian plate and Afghan block (Fig.1; Ahmed and Abbas, 1979). The Waziristan ophiolite occurs in the north of the Zhob ophiolite and comprises crustal sections, well-exposed mantle sections and upper volcano-sedimentary units, that formed in a back-arc basin (Khan, 2000). In the south of the Zhob ophiolite, the Muslim Bagh ophiolite comprises mostly ophiolitic rock units including the crustal section, transition zone, mantle section, lava and metamorphic sole rocks in a back-arc basin setting and hosts chromitite, volcanogenic massive sulfide (VMS), and manganese deposits (Fig. 1; Kakar et al., 2014; Khan et al., 2020 a, b). Further to the south, the Bela ophiolite is found, and this was generated in a supra-subduction zone setting (Ahmed, 1991, 1993). The Katwaz basin occurs in the west of the Zhob ophiolite and is comprised of a thick sequence of shallow marine flysch sediments between the central Afghan block and Indian plate (Cassaigneau, 1979).

Two tectonic blocks: the Zhob valley ophiolite and Katwaz basin are found between the Indian plate and Afghan block. The Zhob ophiolitic blocks in the Zhob Valley are divided into three tectono-stratigraphic rock units: 1) the flysch zone, 2) Zhob ophiolite and 3) the calcareous zone (Naeem et al., 2021, 2022) with the Zhob ophiolite being thrusted over the calcareous zone (Fig.1; Şengor, 1987; Kazmi and Jan, 1997). The Zhob ophiolitic blocks, known as the Naweoba, Ali Khanzai, and Omzha blocks (Jones, 1961) are further divided into six fault-bounded tectonostratigraphic units: a) Hyaloclastite-mudstone unit (Zhm), b) Basalt-chert unit (Zbc), c) Plutonic crustal rocks unit (Zpc), d) Mantle section rocks unit (Zms), e) Metamorphic rocks unit (Zmr), and f) Upper and lower sedimentary rocks unit (Zus and Zls) (Fig.1c,d,e; Naeem et al., 2021).

The rocks of the flysch zone were formed in a fluvial to shallow marine environment in a large sedimentary basin (Trelor and Izatt, 1993). The Nisai Formation of Eocene age unconformably overlies the Zhob ophiolitic blocks (Allemann, 1979). Felsic dyke rocks such as plagiogranite occur in the west of Naweoba, southwest of Ali Khanzai and southeast of Omzha blocks. The Naweoba block is the largest among these blocks with well exposed felsic and mafic dykes. The felsic dykes are found in the plutonic rocks as pods, lenses, and intrusions and occasionally crosscut the ultramafic rocks of Ali Khanzai block in contrast to the Naweoba and Omzha blocks. The Zhob ophiolitic blocks and their underlying and overlying rocks began to form and extend from the continental margin of the Indian subcontinent over the Neo- Tethys Ocean floor and obducted along with the Muslim Bagh ophiolite (Naeem et al., 2021). Studies on the petrography, geochemistry, geology and tectonic setting of the Zhob ophiolitic blocks and their comparison with Waziristan and Muslim Bagh ophiolite suggest that the Zhob ophiolite was also formed at the same time as the formation and emplacement of the Muslim Bagh ophiolite (Naeem et al., 2022).

3. Field Features of Felsic and Mafic Dykes

The felsic (plagiogranite) dykes of the Zhob ophiolite are intruded into the volcanic and plutonic mafic crustal rock units as lenses, pods, pockets, xenoliths and inclusions. The felsic dyke rocks (plagiogranite) are medium to coarse-grained, hard, compact and creamy white to white-green in colour, composed of quartz, plagioclase, apatite, zircon and accessory ferromagnesian minerals such as, biotite and magnetite. The intrusions of felsic dykes in the basal part of the gabbroic rocks in all blocks are common (Fig. 2a, b). Small light gray felsic dyke occurs in the gabbroic section the Omzha block which is intensely tectonized by faults

and shear zones (Fig. 2c). The tectonic inclusions of the felsic and mafic dyke swarms are found in the serpentine mélanges which are derived from fragmented sections of ophiolite (Fig. 2d). In the Ali Khanzai block, parts of the plagiogranite body are highly altered and most of the samples show epidotization (Fig. 2e). significant number of fresh and altered felsic dykes are present in the lower part of the gabbroic rocks near Naweoba Killi in the Naweoba block (Fig. 2f). The felsic rocks are in faulted contact with volcanic and volcanoclastic rocks and are in transitional contact with mafic rocks at several localities in the Zhob ophiolite.

The mafic (dolerite) dykes are light gray to dark gray, fine to medium-grained with variable degrees of alteration. The mafic dykes range in thickness from a few centimeters to five meters and several hundred meters in length. The mafic dykes crosscut the mafic and ultramafic rocks of all three ophiolitic blocks. In the Ali Khanzai block these mafic dykes are not well-exposed and are mostly broken and sheared along with country rocks. The dykes do not show cross-cutting relationships with one another, but joints and fractures are very common. Massive dolerite dyke in Naweoba block intruded in ultramafic rocks (Fig. 3a). Dolerite dyke showing intruded contact with harzburgite in Omzha block of the Zhob ophiolite (Fig. 3b). The dykes in Naweoba block are intruded as massive bodies in gabbroic rocks (Fig. 3c). Hard and compact dolerite dykes intruded in gabbroic rock of the Naweoba block (Fig. 3d). The interaction of dolerite rocks remelted host rocks and formed chilled margin near Shiakhan Killi north of Ali Khanzai block of the Zhob ophiolite (Fig. 3e). Furthermore, the studied dykes are common in the peridotite and make sharp intrusive contacts with peridotite at some localities in the Ali Khanzai block (Fig. 3f). The dolerite dykes are altered and fragmented near Konnai Killi in the south of Omzha Block due to extensive tectonic activity and several concealed faults in the region (Fig. 3g). These dykes commonly exhibit usually intrusive contacts with host peridotite in the Naweoba block (Fig. 3h).

4. Petrography

4.1. Felsic Dykes

The Zhob ophiolite plagiogranite dykes are light grey to creamy white, fine to coarse-grained, and contain abundant quartz, microcline, orthoclase and plagioclase. In thin section the plagiogranite is extremely fractured and quartz is present as clusters that are surrounded by epidote crystals aggregates (Fig. 4a). The quartz grains are fresh and comprised on average 40% of the rock with (35%) plagioclase, with mafic (usually hornblende and pyroxene) minerals

being minor constituents (<10%) and K-feldspar (orthoclase) being a rare phase. A few samples of plagiogranite show large crystals of euhedral to subhedral plagioclase with quartz and minor amphibole (Fig. 4b). Accessory minerals are biotite, amphibole, calcite and opaque minerals. Chlorite, which is the alteration product of biotite and hornblende is present in Zhob ophiolite plagiogranite. Euhedral crystals of zircon with quartz and plagioclase are observed in a few thin sections of plagiogranite from the Naweoba block (Fig. 4c). Most plagioclase feldspar is partially altered. The epidote grains have a partially chloritized rim and sericite is observed as an alteration product of alkali feldspar. Plagiogranite shows massive, subhedral to anhedral, hypidiomorphic and inter-granular texture and anhedral to subhedral crystals of plagioclase with quartz (Fig. 4d). Phenocrysts of plagioclase, quartz, hornblende and pyroxene are surrounded by a fine groundmass composed of plagioclase, quartz, hornblende, pyroxene, potassium feldspar and accessory phases. The plagioclase mostly shows zoning, and pyroxene is partially altered to chlorite (Fig. 4e). Anhedral crystals of quartz have undulose extinction. Plagiogranite from the Ali Khanzai and Omzha blocks has quartz, plagioclase and deformed biotite with inter-grown muscovite (Fig. 4f).

4.2. Mafic Dykes

Dolerite dykes of the Zhob ophiolitic blocks are aphanitic, fine to medium-grained, allotriomorphic, intergranular and have sub-ophitic texture. The dolerite dykes are composed of plagioclase, clinopyroxene, hornblende, magnetite and quartz grains and are chloritized with quartz aggregates (Fig. 5a, b). Clinopyroxene and plagioclase are primary minerals while zeolites, quartz and calcite are secondary minerals. Dolerite rocks are granular and have interlocking contacts between plagioclase and pyroxene crystals (Fig. 5c, d). Plagioclase occurs as phenocrysts and is partially altered to sericite. Sub-ophitic plagioclase phenocrysts occur both as laths and larger anhedral to subhedral prisms (Fig. 5e, f). The plagioclase laths are partially to completely altered to epidote, sericite and calcite and penetrate the hornblende and pyroxene minerals (Fig. 5g, h). The hornblende is commonly altered to chlorite but is replaced by biotite in places. Clinopyroxene is augite which is partly to completely altered to amphibole and magnetite and forms a considerable part of groundmass, while in the rocks from the Naweoba it is present as phenocrysts. In few thin sections of the Ali Khanzai block the augite is anhedral and has faint zoning. The fine-grained quartz aggregates are found among the main minerals. Secondary minerals such as calcite, epidote, chlorite, amphibole and quartz suggest

that the dykes have been subjected to metamorphism under greenschist facies conditions. Tiny, rounded grains of iron oxides fill the interstices between primary minerals while calcite veins occupy fractures in the rock.

5. Analytical Methods

Rock samples of both felsic and mafic dykes from the three ophiolitic blocks of the Zhob ophiolite were analyzed. Samples were powdered to 200mesh after removing the weathered surfaces. Each powder sample was heated for two hours to 900°C in a porcelain crucible to obtain the loss on ignition. Inductively coupled plasma optical emission (ICP-OES) and inductively coupled plasma mass spectrometry (ICP-MS) were used to analyze the major, trace and rare earth elements in the School of Earth and Environmental Sciences, Cardiff University, Wales, UK.

In a platinum crucible 0.4 g of lithium metaborate flux was mixed with 0.1 g ignited sample. A few drops of wetting agents such as lithium iodide were added in each mixture for fusion by using the Claisse Flaxy automated fusion system. The mixture was then dissolved in 30ml of de-ionized water and 20 ml of 10% HNO_3 by using the Milli-Q purification system. When the mixture had fully dissolved, and the solution was made up to 100 ml with 20 de-ionized water then 1 ml of 100 ppm Rh spike was added to the solution. At the end 20 ml of each solution was run on ICP-OES to determine the major element and some trace element abundances. To obtain the abundances of trace elements, 1 ml of each solution was added to 1 ml of In and Tl and 8 ml of 2% HNO_3 was run on the ICP-MS. The instruments used to analyze elements were, a JY von Horiba Ultima 2 ICP-OES and a thermos elemental X7 series ICP-MS at Cardiff University Wales, UK.

6. Results

Five mafic (dolerite) and four felsic (plagiogranite) dyke samples from Zhob ophiolites were analyzed for major, trace and rare earth element geochemistry.

The major oxides from the mafic dykes of the Zhob ophiolite have the following range of compositions: MgO (1.7–5.7 wt.%), CaO (4.0 –14.3 wt.%), TiO_2 (0.3 –1.3 wt.%), Na_2O (0.4 – 6.0 wt.%), K_2O (0.02–1.3 wt.%), SiO_2 (47.6 –56.7 wt.%), Al_2O_3 (12.8 –15.2 wt.%), and Fe_2O_3 (10.7–12.5 wt.%). The range of trace elements are; Sc (8 – 43 ppm); V (11 – 351 ppm),

193 Cr (3 – 39 ppm), Co (3 – 552 ppm), Ni (1 – 501 ppm), Cu (8 – 173 ppm), Zn (15 – 69 ppm),
194 Sr (68 – 799 ppm), Y (16 – 31 ppm), Zr (29 – 77 ppm), and Ba (11 – 238 ppm).

195 The major oxides from the felsic dykes of the Zhob ophiolite have the following
196 compositional range: CaO (0.5 – 18.4 wt.%), TiO_2 (0.03 – 0.2 wt.%), alkalis (Na_2O + K_2O =
197 3.1–10.7 wt.%), MgO (0.1 – 1.3 wt.%), Al_2O_3 (10.1 – 18.2 wt.%), $Fe_2O_3^t$ (0.2 – 1.4 wt.%), and
198 SiO_2 contents (68.9 – 77.9 wt.%). The range of trace elements are; Sc (1 – 21 ppm), V (0 – 30
199 ppm), Cr (1 – 14 ppm); Co (1 – 5 ppm), Ni (2 – 13 ppm), Cu (2 – 4 ppm), Zn (2 – 26 ppm), Sr
200 (59 – 163 ppm), Y (13 – 32 ppm), Zr (23 – 65 ppm), and Ba (8 – 43 ppm).

201 The felsic and mafic dyke samples were plotted on Zr and MgO Harker-type binary
202 diagrams against other major and trace elements to determine fractionation trends of these
203 rocks. On binary plots of the MgO versus other elements, the felsic and mafic dykes show
204 some degree of clustering and scattering (Fig. 6 a, b). Major oxides and trace elements of felsic
205 dykes such as Fe_2O_3, SiO_2, TiO_2, Sr, Nb, and Co versus MgO show clustering while Na_2O,
206 Al_2O_3, CaO, Ni, Zr, and V versus MgO exhibit scattered patterns. Major oxides and trace
207 elements of mafic dykes such as SiO_2, Na_2O, Al_2O_3, Co, and Ni versus MgO show clustering
208 while CaO, TiO_2, Fe_2O_3, Zr, Nd, and Nb versus MgO exhibit scattered patterns. On binary plot
209 of TiO_2 vs. Mg the dolerite dykes of the Zhob ophiolites with high MgO and low TiO_2 show
210 small degrees of fractional crystallization. On the TiO_2 versus Mg plot for dolerite dykes TiO_2
211 increases during fractional crystallization and decreases when the degree of partial melting
212 increases.

213 Binary plots of Zr versus other elements for the felsic and mafic dykes also show some
214 degree of scattering (Fig. 7a, b). The ratio of TiO_2 and Zr on TiO_2 versus Zr plot of dolerite
215 dykes increases during fractional crystallization and decreases when the degree of partial
216 melting increases. On total alkali versus silica (TAS) diagram (Le Bas et al., 1986), two
217 samples of dolerite dykes fall in the field of basaltic andesite, two in trachy-basalt and one in
218 the basalt field while two samples of felsic dykes fall in the dacite field and two samples fall
219 in rhyolite field (Fig. 8a). On an immobile trace element Th versus Co diagram (after Hastie et
220 al. 2007) the dolerite rocks plot in the basalt to dacitic – rhyolitic field (Fig. 8b). The felsic
221 rocks were plotted on K_2O vs SiO_2 a diagram and indicate that these rocks are plagiogranites
222 and calc-alkaline in composition (Fig. 9a, b). The Y versus Nb diagram (Pearce et al., 1984),
223 (Fig. 9c) classify these felsic rocks as volcanic arc granites (VAG) or ocean ridge granites
224 (ORG). A volcanic arc setting is also confirmed by the Y versus Nb/Th plot (Jenner et al.,

1991), (Fig. 9d). La-SiO_2 diagram (Brophy, 2009) suggests melting of a depleted source region for these felsic/mafic dyke rocks (Fig. 10).

The dolerite dyke samples fall in basalt andesite and basalt field when plotted on Nb/Y versus Zr/Ti diagram of Pearce (1996), (Fig. 11a). On Zr versus P_2O_5 and Nb/Y versus Ti/Y diagrams (Winchester and Floyd, 1976; Pearce, 1982), (Fig. 11 b, c) the dolerite rock samples classify as N-MORB and arc rocks. Similarly, on Ti versus Zr (Pearce, 1981), Y versus Nb/Th (Jenner et al., 1991) and V versus Ti diagrams (Shervais, 1982), these mafic dyke rocks plot as N-MORB and IAT or BAB (Fig. 11d, e, f). The Na_2O vs K_2O diagram (Fig. 10g) confirms the sodic composition of rocks while the Ba versus Zr plot (Saunders and Tarney, 1991) further indicate their BABB and N-MORB type nature (Fig. 11h). Triangular $MnO/TiO_2/P_2O_5$ diagram (Mullen 1983) conform the tholeiitic nature of these mafic rocks (Fig. 11i). On an N-MORB normalized plot (Sun and McDonough, 1989), both the plagiogranite felsic and dolerite mafic dykes have flat high field strength (HFS) element patterns parallel to N-MORB (Fig. 12a), while the large ion lithophile (LIL) elements are more enriched than N-MORB (Fig. 13a). On chondrite normalized diagrams (Fig. 12b and13b), the REE patterns of these dykes are almost flat like those of N-MORB with slight enrichment in LREE and negative Eu anomalies. The enrichment of LILEs may be due to either alteration or addition through adding a slab derived hydrous component to the melt source region, i.e. a depleted mantle wedge. However, the positive anomaly of Th and negative anomaly of Nb relative to other incompatible elements in the NMORB-normalized plots support the latter possibility (Wood, 1980). The flat pattern of both the LREEs and the HREEs of the dyke suggest derivation from a depleted mantle source.

7. Discussion

Plagiogranites that contain more than 15 wt.% Al_2O_3 were likely generated in a continental setting whereas those containing less than 15 wt.% Al_2O_3 are considered to have been formed in an oceanic ridge setting (Arth, 1979; Pearce et al., 1984). The felsic dykes of the Zhob ophiolite contain less than 15 wt.% Al_2O_3 are oceanic plagiogranite. The Zhob plagiogranite dyke rocks are calc-alkaline in composition and fall below the line of partial melting of depleted source that formed in volcanic arc setting. The dolerite dyke rocks of the Zhob ophiolitic are basaltic to basalt-andesite in composition with low concentrations of TiO_2 and P_2O_5 and so are tholeiitic. The P_2O_5 versus Zr diagram and Ti/Y versus Nb/Y diagram further confirm the tholeiitic composition of these dolerite rocks. The dolerite dykes on Ti versus Zr, Nb/Th versus Y, V versus T, Ba versus Zr, $TiO_2/MnO/P_2O_5$ diagrams and the large

ion lithophile (LIL) elements are more enriched than N-MORB while high field strength (HFS) elements show a flat pattern parallel to N-MORB on an N-MORB normalized plot and suggest that these dykes are transitional between IAT and MORB. The enrichment of LIL elements over the high field strength (HFS) elements and depletion in Nb indicate an arc-related origin (Tankut et al., 1998; Dilek et al., 2006; Robinson et al., 2008). This is explained by the addition of a hydrous slab derived component to a depleted mantle wedge (Thirlwall et al. 1996). The crustal part of the Zhob ophiolite has a less-well developed gabbroic section with a relatively thick ultramafic-mafic cumulate section and geochemical signatures that indicate an island arc or supra-subduction setting (Naeem et al., 2022). The REE patterns of both felsic and mafic dykes are almost flat like those of N-MORB with slight enrichment in LREE and negative Eu anomalies on chondrite diagrams. The normalized REE and trace diagrams further indicate the transitional character of these felsic and mafic dykes between N-MORB and IAT and the enrichment of LIL element and depletion of Nb suggest supra subduction zone tectonic setting.

7.1 Petrogenesis

The bulk chemical compositions of the plagiogranites are similar to granite and rhyolite but plagiogranite contains K_2O <1% while granite and rhyolite contain K_2O >3%. The felsic dyke rocks of the Zhob ophiolite with low TiO_2, MgO and K_2O concentrations (<1 wt.%) and high SiO_2, Al_2O_3 and Na_2O are considered a key characteristic of oceanic plagiogranites that have been derived by partial melting, as opposed to oceanic plagiogranites derived through fractional crystallization that display higher TiO_2 contents (>1 wt.%; Koepke et al., 2004, 2007).

Oceanic plagiogranite can be formed by fractional crystallization of sub-alkaline tholeiitic magma (Cox et al., 2019; Grimes et al., 2011) or partial melting of crustal rocks under hydrous conditions (Barker, 1979) or by liquid immiscibility or metasomatism (Dixon and Rutherford, 1979). On binary plots the major oxides and trace elements of felsic dykes such as Fe_2O_3, SiO_2, TiO_2, Sr, Nb, and Co versus MgO show clustering while Na_2O, Al_2O_3, CaO, Ni, Zr, and V versus MgO exhibit scattered patterns which indicate the fractional crystallization process (Fig. 6a, 7a).

The plagiogranites of the Zhob ophiolite show their own distinct field (Fig.6a, 7a) which indicates that they are not related to the other units by simple fractional crystallization processes. The Zhob ophiolite sequence is mostly mafic, ultramafic and felsic rocks with the absence of intermediate composition rocks, which indicate the fractional crystallization process

for the origin of the plagiogranite by a basic parental melt. Moreover, the SiO_2 range of the plagiogranites would suggest that fractional crystallization did not play a significant role in their petrogenesis. On chondrite normalized diagrams (Fig. 12b), the enrichment of La, Ce, Pr and concave-upwards patterns displayed by the plagiogranites support a role for amphibole during their petrogenesis, due to amphiboles preference for MREE over LREE and HREE (Davidson 2012). The enrichment of La, Ce and Pr does not indicate whether amphibole was crystallizing from a parental magma or acting as a residual phase during the fusion of a mafic protolith. An origin by silicate–liquid immiscibility (Dixon and Rutherford, 1979) is unlikely for the Zhob ophiolite plagiogranites. This is evidenced by the absence of the associated immiscible Fe-rich liquid (as Fe-rich mafic units) from the Zhob ophiolite.

The Zhob plagiogranite dykes with high SiO_2 and low TiO_2 suggest that they were derived by partial melting of gabbroic rocks in the crustal sequence. The Brophy (2009) model on the behavior of REEs and SiO_2 was used to determine the petrogenesis of felsic rock of the Zhob ophiolite (Fig. 10). It is estimated that almost 70% felsic rocks within ophiolite complexes were generated by partial melting of depleted basalts or gabbros (Furnes and Delik, 2017). Based on geochemical characteristics and petrogenetic models, the Zhob plagiogranite dykes were formed as a result of high degrees of partial melting in the presence of water from subduction.

The mafic dykes of the Zhob ophiolite with high contents of LILEs and the flat pattern of the HFSEs and REEs, with no depletion in the LREEs are indicative of an IAT signature (Figure 12a, 13a). The enrichment of LILEs may be due to either alteration or addition of a slab derived hydrous component to the melt source region, i.e. a depleted mantle wedge. However, the positive anomaly of Th and negative anomaly of Nb relative to other incompatible elements in the NMORB-normalized plots support the latter possibility (e.g. Wood, 1980; Hofmann, 1997). The flat pattern of both the LREEs and the HREEs (with the exception of elements La and Ce) of the dolerite dyke suggest derivation from a depleted mantle source. The mafic rocks of the Zhob ophiolite (basalt and gabbro) have very low contents of La and the plagiogranite and diorite samples plot below the line of partial melting of a highly depleted source with no indication of derivation by fractional crystallization (Fig. 10). Hence, both felsic and mafic dyke rocks of the Zhob ophiolite are likely derived from partial melting of a depleted source.

7.2 Tectonic Setting

The Zhob, Muslim Bagh and Waziristan ophiolites plagiogranite dykes (Khan, 2000; Kakar et al., 2014) have K_2O and SiO_2 relationships, which suggest that these rocks were formed in oceanic tectonic setting. The Muslim Bagh Ophiolite formed ~80.2 ± 1.5 Ma ago (Kakar et al. 2012) in a supra-subduction zone tectonic setting related to the west–northwest dipping subduction (Gnos et al., 1997) of a narrow branch of the Neo-Tethys Ocean (Mahmood et al., 1995; Kakar et al., 2014). Various plots based on LIL elements and HFS elements, e.g., Fig. 8c and d, suggest that the plagiogranite dykes of the Zhob, Muslim Bagh and Waziristan ophiolites are transitional between volcanic arc granite (VAG) and oceanic ridges granite (ORG). The Nb content of volcanic arc granite (VAG) is less than 15 ppm while in plate granite (WPG) it is more than 15 ppm. The N-MORB normalized pattern of the Zhob plagiogranite shows LREE enrichment relative to HREE with very slight negative Nb and Ta anomalies and a marked depletion in Ti with a positive Th anomaly (Fig. 12a), which indicate that these rocks were generated in N-MORB and island arc settings and are supportive of a supra-subduction zone environment. Volcanic arc plagiogranites are chemically indistinguishable from back arc basin (Supra-subduction) plagiogranites (Pearce et al., 984). Low TiO_2 contents (0.03 wt. %) and Nb depletion in plagiogranite dyke samples of the Zhob ophiolite indicate a back-arc setting. The Zhob ophiolite dolerite dykes' rocks are transitional between island arc and mid oceanic basalt that disproves a typical mid-ocean ridge origin for these dykes. The depletion of Nb and enrichment of the LILE over the HFSE suggest the involvement of a subduction fluid component in the source region and suggest that both the felsic and mafic dykes are formed in a back-arc basin or supra-subduction zone setting.

8 Conclusions

1. The Zhob ophiolite contains plagiogranite and dolerite dykes. The felsic dykes are intruded in gabbroic bodies of ultramafic and mafic rock unit as patches, pods and intrusions. The mafic dykes crosscut the whole sequence of the ophiolite and their relationship indicates that the emplacement of the dyke swarms postdated the formation of the Zhob ophiolite.
2. The felsic plagiogranite dykes of the Zhob ophiolite are calc-alkaline oceanic plagiogranites while dolerite dykes are tholeiitic and basaltic in composition.
3. The low value of REEs and positive Eu anomaly indicates that these felsic dykes are formed by partial melting of basic rocks under hydrous conditions. The mafic dyke swarms are derived from an undepleted mantle source.

4. The enrichment of the LILE over the HFSE and the slight depletion of Nb suggest that both dyke swarms of the Zhob ophiolite are formed in a back-arc basin or supra-subduction zone setting.

Acknowledgments

This research was part of the PhD thesis project of Mr. Abdul Naeem PhD Scholar enrolled in Centre of Excellence in Mineralogy, University of Balochistan, Quetta, Pakistan. Authors are thankful for constructive comments of Dong Liu and two anonymous reviewers which improved manuscript

References

Ahmed Z. (1991) A supra-subduction origin of the Bela ophiolite indicated by acidic rocks, Khuzdar District, Pakistan. *Acta Mineralogica Pakistanica* 5:9–24.

Ahmed Z. (1993) Leucocratic rocks from the Bela ophiolite, Khuzdar District, Pakistan. In: Treloar PJ, Searle MP (eds) Himalayan tectonics. *Geological Society of London Special Publicaions* 74:89–100.

Ahmad Z., Abbas S.G. (1979) The Muslim Bagh Ophiolites. In *Geodynamics of Pakistan* (eds A. Farah., A. DeJong), pp. 243–51. Pakistan: Geological Survey of Pakistan.

Allemann F. (1979) Time of emplacement of the Zhob Valley ophiolite and Bela ophiolite, Balochistan (preliminary report). In: Farah, A., Dejong, K.A. (Eds.), Geodynamics of Pakistan. *Geological Survey of Pakistan*, Quetta, pp. *213*–242.

Arth J.G. (1979) Some trace elements in trondhjemites their implications to magma genesis and paleo tectonic setting. In: Barker F (ed) Trondhjemites, Dacite, and Related Rocks. Elsevier, Amsterdam, pp 123-132. https://doi.org/10.1016/B978-0-444-41765-7.50008-3

Arndt N.T., Coltice N., Helmstaedt H., Gregoire M. (2009) Origin of Archean subcontinental lithospheric mantle: Some petrological constraints. *Lithos* 109: 61–71. https://doi.org/10.1016/j.lithos.2008.10.019

Barker F. (1979) Trondhjemites: definition, environment and hypothesis of origin. In Trondhjemites, Dacites, and Related Rocks (ed. F. Barker), pp. 1–12. Amsterdam: Elsevier. https://doi.org/10.1016/B978-0-444-41765-7.50006-X

Beccaluva L., Chinchilla-Chaves A. L., Coltorti M., Giunta G., Siena F., Vaccaro C. (1999) Petrological and structural significance of the Santa Elena-Nicoya ophiolitic complex in Costa Rica and geodynamic implications. *European Journal of Mineralogy* 11: 1091–1107.

Brophy J.G. (2009) La-SiO_2 and Yb-SiO_2 systematics in mid-ocean ridge magmas: implications for the origin of oceanic plagiogranite. *Contributions to Mineralogy and Petrology* 158: 99-111. https://doi.org/10.1007/s00410-008-0372-3

Brophy J.G., Pu X. (2012) Rare earth element–SiO_2 systematics of mid-ocean ridge plagiogranites and host gabbros from the Fournier oceanic fragment, New Brunswick, Canada. *Contributions to Mineralogy and Petrology* 164: 191–204. https://doi.org/10.1007/s00410-012-0732-x

Cassaingeau C. (1979) Contribution al'étude des sutures Inde-Eurasie, la zone de suture de Khostdans le Sud-Est de l'Afghanistan. L'Obduction Paleocene et la tectoniquetertiaire. Unpublished Ph. D dissertation, Montpellier, France 145.

Coleman R.G., Peterman Z.E. (1975) Oceanic plagiogranite. *Journal of Geophysical Research* 1099– 108. https://doi.org/10.1029/JB080i008p01099

Cox D., Kerr A.C., Hastie A.R., Kakar M.I. (2019) The petrogenesis of small volume plagiogranites in the Muslim Bagh Ophiolite, northwestern Pakistan: Implications for the generation of Archaean juvenile continental crust. *Geological Magazine* 156 (5): 874–888. https://doi.org/10.1017/S0016756818000250

Davidson J., Turner S., Plank T. (2012) Dy/Dy∗: Variations arising from mantle sources and petrogenetic processes. *Journal of Petrology* 54: 525–37. https://doi.org/10.1093/petrology/egs076

Dilek Y., Thy P., Hacker B., Grundvig S. (2006) Structure and petrology of Tauride ophiolites and mafic dyke intrusions (Turkey): implications for the Neotethyan *Ocean. Geological Society of America* 111: 1192–1216. https://doi.org/10.1130/0016-7606(1999)111<1192:SAPOTO>2.3.CO;2

Dilek Y., Furnes H. (2011) Ophiolite genesis and global tectonics: geochemical and tectonic fingerprinting of ancient oceanic lithosphere. *Geological society of America Bulletin* 123:387–411. https://doi.org/10.1130/B30446.1

Dixon S., Rutherford M.J. (1979) Plagiogranites as late-stage immiscible liquids in ophiolite and midocean ridge suites an experimental study. *Earth and Planetary Science Letters* 45: 45–60. https://doi.org/10.1016/0012-821X(79)90106-7

France L., Koepke J., Ildefonse B., Cichy S.B., Deschamps F. (2010) Hydrous partial melting in the sheeted dike complex at fast spreading ridges: experimental and natural observations. *Contributions to Mineralogy and Petrology* 160: 683–704. https://doi.org/10.1007/s00410-010-0502-6

Furnes H., Dilek Y, (2017) Geochemical characterization and petrogenesis of intermediate to silicic rocks in ophiolites: A global synthesis. *Earth-Science Reviews* 166:1-37. https://doi.org/10.1016/j.earscirev.2017.01.001

Gansser A. (1979) Reconnaissance visits to the ophiolites in Balochistan and the Himalaya. In: Farah A, DeJong KA (eds) Geodynamics of Pakistan. *Geological Survey of Pakistan* 206–209.

Gnos E., Immenhauser A., Peters T.J. (1997) Late Cretaceous/early Tertiary convergence between the Indian and Arabian plates recorded in ophiolites and related sediments. *Tectonophysics* 271: 1–19. https://doi.org/10.1016/S0040-1951(96)00249-1

Grimes C.B., Ushikubo T., John B.E., Valley J.W. (2011) Uniformly mantle-like Delta18O in zircons from oceanic plagiogranites and gabbros. *Contributions to Mineralogy and Petrology* 161: 13–33. https://doi.org/10.1007/s00410-010-0519-x

Hastie A.R., Kerr A.C., Pearce J.A., Mitchell S.F. (2007) Classification of altered volcanic island arc rocks using immobile trace elements: development of the Th–Co discrimination diagram. *Journal of Petrology* 48: 2341–2357. https://doi.org/10.1093/petrology/egm062

Hofmann A.W (1997) Mantle geochemistry: the message from oceanic volcanism. *Nature* 385: 219–229. https://doi.org/10.1038/385219a0

Jenner G.A., Dunning G.R., Malpas J., Brown M., Brace T. (1991) Bay of Islands and Little Port complexes revisited: age, geochemical and isotopic evidence confirm supra-subduction zone origin. *Canadian Journal Earth Sciences* 28:135–162. https://doi.org/10.1139/e91-146

Jones A.G. (1960) Reconnaissance Geology of Part of West Pakistan. A Colombo Plan Cooperative Project, Government of Canada, Toronto, 550.

Kakar M.I. (2012) Petrology, geochemistry and tectonic setting of the Muslim Bagh ophiolite, Balochistan, Pakistan. PhD Thesis (unpublished) Centre of Excellence in Mineralogy, University of Balochistan, Quetta, Pakistan.

Kakar M.I., Kerr A.C., Mahmood K., Collins A.S., Khan M., McDonald I. (2014) Supra-subduction zone tectonic setting of the Muslim Bagh ophiolite, northwestern Pakistan:

insights from geochemistry and petrology. *Lithos* 202-203:190–206. https://doi.org/10.1016/j.lithos.2014.05.029

Korenaga J. (2013) Initiation and evolution of plate tectonics on Earth: Theories and observations. *Annual Review Earth and Planetary Sciences* 41: 117–151. 10.1146/annurev-earth-050212-124208

Kazmi A.H., Jan M.Q. (1997) Geology and Tectonics of Pakistan. Graphic Publishers, Pakistan.

Khan S.R. (2000) Petrology and geochemistry of a part of Waziristan Ophiolite, NW Pakistan. Unpublished PhD thesis, University of Peshawar 253.

Khan S.R., Jan M.Q., Khan M.A., Khan T. (2001) Geochemistry and petrogenesis of the sheeted dykes from Waziristan ophiolite, NW Pakistan and their tectonic implications. Abstract: 16th HKT Workshop, Graz, Austria. *Journal of Asian Earth Sciences* 19(3A): 36.

Khan M. A., Kakar M. I., Ulrich T., Ali L., Kerr A. C., Mahmood K., Siddiqui R.H. (2020a) Genesis of Manganese Deposits in the Ali Khanzai Block of the Zhob Ophiolite, Pakistan: Inferences from Geochemistry and Mineralogy. *Journal of Earth Science* 31(5): 884-895. https://doi.org/10.1007/s12583-020-1337-3

Khan M.A., Ulrich T., Kakar M.I., Akmaz R.M., Siddiqui R.H., Ali. L. (2020b) Genesis and geotectonic setting of podiform chromitites from the Zhob Valley Ophiolite, Pakistan: inferences from chromite composition. *Episodes* 43(4):10-1039. https://doi.org/10.18814/epiiugs/2020/020065

Klein E.M., Langmuir C.H. (1987) Global correlations of ocean ridge basalt chemistry with axial depth and crustal thickness. *Journal of Geophysical Research* 92: 8089–8115. https://doi.org/10.1029/JB092iB08p08089

Koepke J., Berndt J., Feig S. T., Holtz F. (2007) The formation of SiO2-rich melts within the deep oceanic crust by hydrous partial melting of gabbros. *Contributions to Mineralogy and Petrology* 153: 67–84. https://doi.org/10.1007/s00410-006-0135-y

Koepke J., Feig S. T., Snow J., Freise M. (2004) Petrogenesis of oceanic plagiogranites by partial melting of gabbros: an experimental study. *Contributions to Mineralogy and Petrology* 146: 414–432. https://doi.org/10.1007/s00410-003-0511-9

LeBas M. J., LeMaitre R.W., Streckeisen A., Zanettin B. (1986) A chemical classification of volcanic rocks based on the total alkali silica diagram. *Journal of Petrology* 27: 745–750. https://doi.org/10.1093/petrology/27.3.745

Mahmood K., Boudier F., Gnos E., Monié P., Nicolas A. (1995) 40Ar/39Ar dating of the emplacement of the Muslim Bagh ophiolite, Pakistan. *Tectonophysics* 250: 169–181. https://doi.org/10.1016/0040-1951(95)00017-5

Middlemost E.A. (1994) Naming materials in the magma/igneous rock system. *Earth Science Reviews* 37:215–224. https://doi.org/10.1016/0012-8252(94)90029-9

Mullen E. D. (1983) $MnO/TiO_2/P_2O_5$: a minor element discriminant for basaltic rocks of oceanic environments and its implications for petrogenesis. *Earth and Planetary Science Letters* 62(1): 53–62. https://doi.org/10.1016/0012-821X(83)90070-5

Naeem A., Kerr A.C., Kakar M.I., Siddiqui R.H., Khan M.A., Ahmed N. (2021) Petrology and geochemistry of volcanic and volcanoclastic rocks from Zhob ophiolite, North-Western Pakistan. *Arabian Journal of Geosciences* 14:97. https://doi.org/10.1007/s12517-020-06352-0

Naeem A., Kakar M.I., Siddiqui R.H., Kerr A.C., Jan M.Q., Khan M.A. (2022) Geology and petrogenesis of gabbro from the Zhob Ophiolite, Balochistan, Pakistan. *Arabian Journal of Geosciences* 15:1205 https://doi.org/10.1007/s12517-022-10417-7

Pearce J.A., Lippard S.J., Roberts S. (1984) Characteristics and tectonic significance of supra-subduction zone ophiolites. *Geological Society of London Special Publication* 16: 74–94. https://doi.org/10.1144/gsl.sp.1984.016.01.06

Pearce J.A. (1996) A user's guide to basalt discrimination diagrams. In: Bailes AH, Christiansen EH, Galley AG, Jenner GA, Keith Jeffrey D, Kerrich R, Lentz David R, LesherCM, Lucas Stephen B, Ludden JN, Pearce JA, Peloquin SA, Stern RA, Stone WE, Syme EC, Swinden HS, Wyman DA (eds) Trace element geochemistry of volcanic rocks; applications for massive sulphides exploration, short course notes, *Geological Association of Canada* 12:79–113

Pearce J.A. (1982) Trace elements characteristics of lavas from destructive plate boundaries. In: Throp RS (ed) Andesites: orogenic andesites and related rocks. John Wiley and Sons, New York 525–548

Pearce J.A., Alabaster T., Scheton A.W., Searle M.P. (1981) The Oman ophiolite as a cretaceous arc-basin complex: evidence and implications: *Philosophical transactions Royal Society of London* 299–317. https://doi.org/10.1098/rsta.1981.0066

Robertson A.H. (2002) Overview of the genesis and emplacement of Mesozoic ophiolites in the Eastern Mediterranean Tethyan region. *Lithos* 65(1):1–67. https://doi.org/10.1016/S0024-4937(02)00160-3

515 Robinson P.T., Malpas J., Dilek Y., Zhou M. (2008) The significance of sheeted dike complexes
516 in ophiolites. *Geological Society of America Today* 18: 4–10.
517 Sengor A.M.C. (1987) Mid-Mesozoic closure of Permo-Triassic Tethys and its implications.
518 *Nature* 279: 590–593. https://doi.org/10.1038/279590a0
519 Shervais J.W. (1982) Ti-V plots and the petrogenesis of modern and ophiolitic lavas. *Earth and*
520 *Planetary Science Letters* 32; 114-120. https://doi.org/10.1016/0012-821X(82)90120-0
521 Sun S.S., McDonough W.F. (1989) In: Saunders A. D., Norry M. J. (eds). Chemical and isotope
522 systematics of oceanic basalts: implications for mantle composition and processes:
523 magmatism in the Ocean Basins. *Geological Society of London Special Publication* 42:
524 313–345. https://doi.org/10.1144/gsl.sp.1989.042.01.19
525 Saunders A.D., Tarney J. (1991) Back-arc basins. In: Floyd, P.A. (eds) Oceanic Basalts.
526 Springer, Dordrecht. https://doi.org/10.1007/978-94-011-3042-4_10
527 Tankut A., Dilek Y., Onen P. (1998) Petrology and geochemistry of the Neo-Tethyan
528 volcanism as revealed in the Ankara mélange, Turkey. *Journal of Volcanology and*
529 *Geothermal Research* 85(1-4): 265-284. https://doi.org/10.1016/S0377-0273(98)00059-6
530 Thirlwall M.F., Graham A.M., Arculus R.J., Harmon R.S., Macpherson C.G. (1996)
531 Resolution of the effects of crustal assimilation, sediment subduction, and fluid transport
532 in island arc magmas; Pb-Sr-Nd-O isotope geochemistry of Grenada, Lesser Antilles:
533 *Geochimica et Cosmochimica Acta* 60(23):4785–4810. https://doi.org/10.1016/S0016-
534 7037(96)00272-4
535 Treloar P.J., Izatt C.N. (1993) Tectonic of the Himalayan collision zone between the Indian
536 plate and the Afghan Blok; a synthesis. In: Treloar PJ, Searle MP (eds) Himalayan
537 tectonics. *Geological Society of London Special Publication* 74: 69–87.
538 https://doi.org/10.1144/gsl.sp.1993.074.01.06
539 Wanless V.D., Perfit M.R., Ridley W.I., Klein E., (2010) Dacite petrogenesis on mid-ocean
540 ridges: evidence for oceanic crustal melting and assimilation. *Journal of Petrology* 51:
541 2377–2410. https://doi.org/10.1093/petrology/egq056
542 Winchester J.A, Floyd P.A. (1976) Geochemical magma type discrimination, application to
543 altered and metamorphosed basic igneous rocks. *Earth and Planetary Science Letters* 28:
544 459–469. https://doi.org/10.1016/0012-821X(76)90207-7
545 Wood D.A. (1980) The application of a Th–Hf–Ta diagram to problems of tectono-magmatic
546 classification and to establishing the nature of crustal contamination of basaltic lavas of

the British tertiary volcanic province. *Earth and Planetary Science Letters* 50: 11–30. https://doi.org/10.1016/0012-821X(80)90116-8

Figures and Tables

Figure 1. (**a**) Geotectonic map of the western and north-western boundary of the Indian Plate with Afghan Block showing the ophiolites occurrences (**b**) shows Khanozai, Muslim Bagh and Zhob Ophiolites and surrounding sedimentary rocks (**c, d and e**) Geological map of Naweoba, Omzha blocks and Ali Khanzai blocks of the Zhob ophiolite. BO; Bela Ophiolite, KO; Khanozai Ophiolite, MO; Muslim Bagh Ophiolite, ZO; Waziristan Ophiolite, ZO; Zhob Ophiolite, DO; Dargai Ophiolite, CO; Chilas Ophiolite, CF; Chaman Fault, PS; Penjwai Suture, HF; Herat Fault, KB; Karakorum Block; MMT; Main Mantle Thrust; MBT; Main Boundary Thrust (modified after Jones, 1961; Naeem et al, 2021).

Figure 2. Field photographs showing, **(a)** a network of felsic veins **(b)** plagiogranite intruding gabbroic rock the intruded in the gabbroic rocks of the Zhob ophiolite **(c)** granitic rock intrusion in mafic rocks in the south of Yaseenzai Killi of the Omzha block **(d**) plagiogranite inclusions in serpentine mélanges **(e)** highly altered plagiogranite body in the Ali Khanzai block near Babar Killi **(f)** large intrusion of plagiogranite bodies in plutonic rocks near Naweoba Killi in Naweoba block

Figure 3. Field photographs showing, (**a**) dolerite dykes in ultramafic rocks in Naweoba block (**b**) in Omzha block (**c**) dolerite dykes (**d**) close-up view of dolerite dykes in gabbroic rocks in Naweoba block (**e**) chilled margin of dolerites near the Shiakhan Killi north of Ali Khanzai block (**f**) sharp intrusive contact of dolerite dykes with peridotite rocks in Ali Khanzai block (**g**) dolerite dykes near Konni Killi south of Omzha Block (**h**) dolerite rocks in dunite and harzburgite in Naweoba block.

Figure 4. (a) plagiogranite showing subhedral quartz surrounded by epidote aggregates (XPL) **(b)** plagiogranite with large crystals of euhedral to subhedral plagioclase with quartz and minor amphibole (XPL) **(c)** plagiogranite containing plagioclase, quartz, minor clinopyroxene and euhedral crystals of zircon (XPL) **(d)** massive plagiogranite with subhedral to anhedral, hypidiomorphic and inter-granular texture and anhedral to subhedral crystals of plagioclase with quartz (XPL) **(e)** clinopyroxene in the plagiogranite partially altered to chlorite (XPL). (**f**) plagiogranite showing quartz, plagioclase and deformed biotite with inter-grown muscovite (XPL).

Figure 5. (a and b) Naweoba block dolerite dyke with sub ophitic texture and shows chloritization and fine quartz aggregates (a. PPL, b. XPL) **(c and d)** Omzha block dolerite dyke showing granular and interlocking contacts between plagioclase and pyroxene crystals (c. PPL, d. XPL). **(e and f)** Ali Khanzai block dolerite dyke with anhedral to subhedral plagioclase phenocrysts and augite phenocrysts with chloritization (e. PPL, f. XPL) **(g and h)** plagioclase laths penetrating pyroxene and hornblende (g. PPL, h. XPL).

Figure 6. (a) Diagrams of MgO versus representative major and trace elements of the felsic dykes (blue) **(b)** diagrams of MgO versus selected major and trace elements of the mafic dykes (yellow) of the Zhob ophiolite. The analyses from the Muslim Bagh and Waziristan ophiolites are taken from (Kakar et al., 2014; Khan, 2000) respectively.

Figure 7. (a) Diagrams of Zr versus representative major and trace elements of the felsic dykes (blue) **(b)** diagrams of Zr versus selected major and trace elements of the mafic dykes (orange) of the Zhob ophiolite. The analyses from the Muslim Bagh and Waziristan ophiolites are taken from Kakar et al. (2014) and Khan, (2000). respectively.

Figure 8. (a) Total alkali versus SiO_2 plot of the mafic dolerite dykes (yellow), (after Le Bas et al., 1986). **(b)** Classification of altered mafic dolerite dykes (yellow) of Zhob ophiolite using the Th–Co classification diagram (immobile trace elements) (after Hastie et al., 2007). The analyses from the Muslim Bagh and Waziristan ophiolites are taken from Kakar et al. (2014) and Khan, (2000), respectively.

Figure 9. (a) Tectonic discrimination plots of the Zhob ophiolite granite SiO_2 versus K_2O plot (after Coleman and Peterman, 1985) **(b)** Co versus Th classification of altered granite using immobile trace elements (after Hastie et al., 2007) **(c)** Nb versus Y plot diagram (Pearce et al., 1984) **(d)** Nb/Y versus Y tectonic discrimination diagram (after Jenner et al., 1991). The analyses from the Muslim Bagh and Waziristan ophiolites are taken from Kakar et al. (2014) and Khan, (2000), respectively.

Figure 10. Felsic rocks and diorite dykes of the Zhob ophiolite are shown on La-SiO_2 diagram which is used to help determine the partial melting and fractional crystallization trend (Modified after Brophy, 2009).

Figure 11. (a) Tectonic discrimination diagram of mafic dolerite dykes (yellow) on Zr/Ti versus Nb/Y (after Pearce, 1996) **(b)** Zr/P_2O_5 versus TiO_2 diagram (after Winchester and Floyd, 1976) **(c)** Nb/Y versus Ti/Y diagram (after Pearce, 1982) **(d)** Zr versus Ti diagram (after Pearce et al., 1981) **(e)** Nb/Y versus Y tectonic discrimination diagram (after Jenner et al., 1991) **(f)** Ti versus V diagram (after Dilek et al., 2011) **(g)** Na_2O versus K_2O diagram (after Middlemost, 1975) **(h)** $MnO/TiO_2/P_2O_5$ triangular diagram (after Mullen, 1983) **(i)** Ba versus Zr tectonomagmatic discrimination diagram (after Saunders and Tarney, 1991). The analyses of the Muslim Bagh and Waziristan ophiolites are taken from Kakar et al. (2014) and Khan, (2000), respectively.

Figure 12. (a) Multi-element N-MORB normalized diagram of the felsic granite dykes (blue) of the Zhob ophiolite **(b)** chondrite normalized REE diagrams of the felsic granite dykes (blue) of the Zhob ophiolite (after Sun and McDonough, 1989). The analyses from the Muslim Bagh ophiolite are taken from Kakar et al., (2014).

Figure 13. (a) Multi-element N-MORB normalized diagram of the mafic dolerite dykes (yellow) of the Zhob ophiolite **(b)** chondrite normalized REE diagrams of the mafic dolerite dykes (yellow) of the Zhob ophiolite (after Sun and McDonough, 1989). The analyses from the Muslim Bagh ophiolite are taken from Kakar et al., (2014).

Table 1. Major oxides (wt %), trace and REE elements (ppm) of the dolerite and plagiogranite dykes of the Zhob ophiolite.

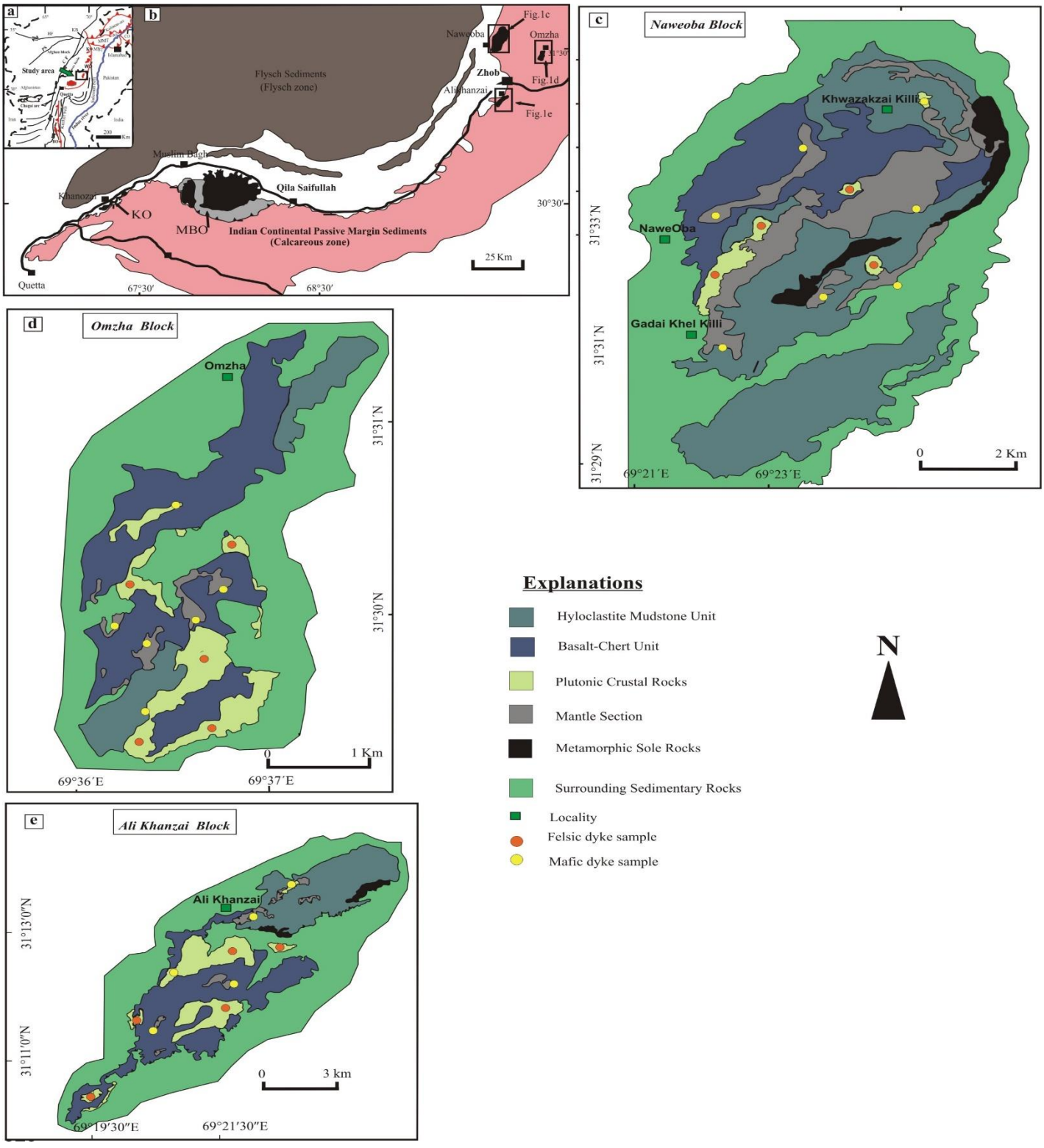

630

631 **Figure 1.**

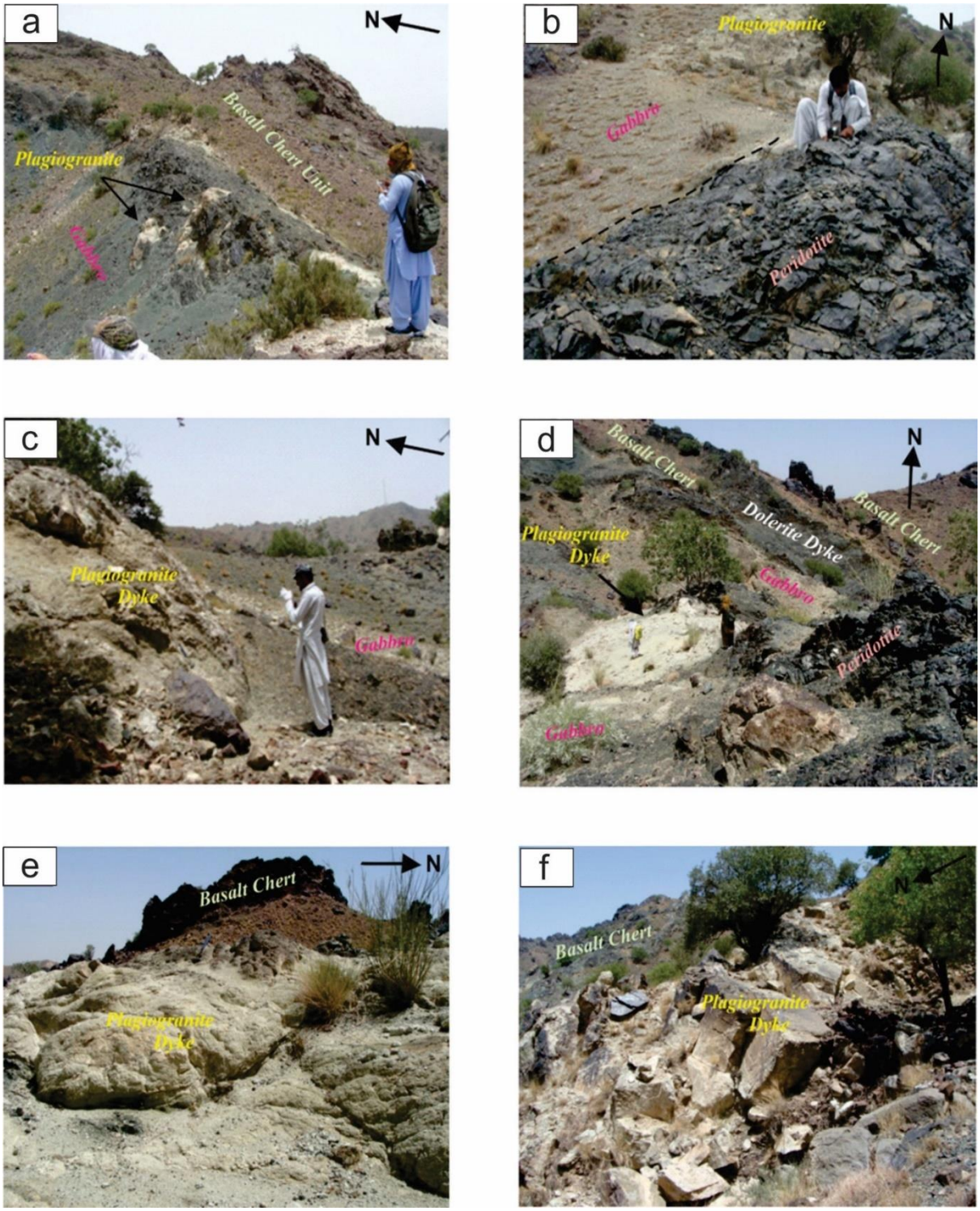

632

633 **Figure 2.**

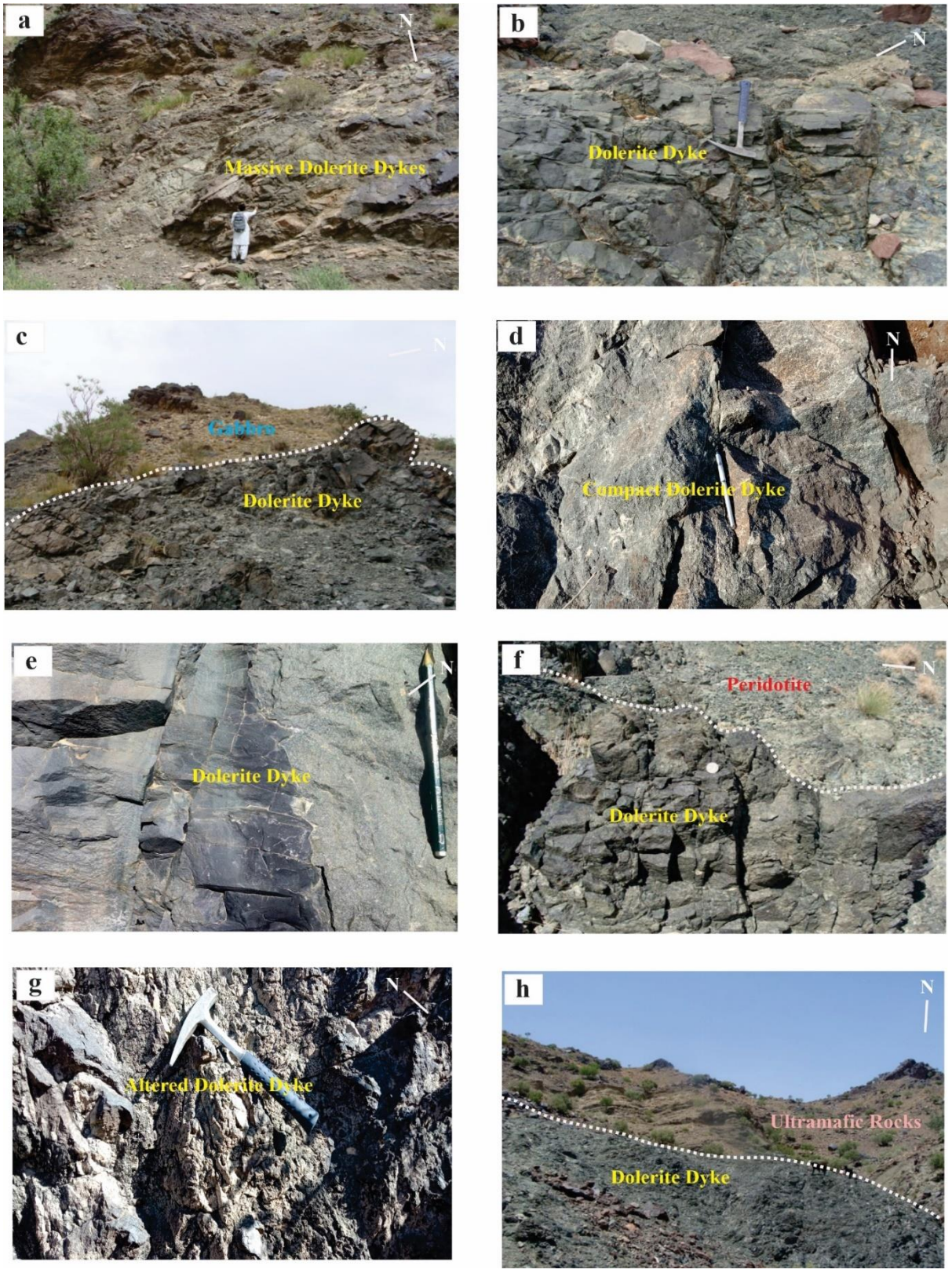
a
N
Massive Dolerite Dykes
b
N
Dolerite Dyke
c
N
Gabbro
Dolerite Dyke
d
N
Compact Dolerite Dyke
e
N
Dolerite Dyke
f
N
Peridotite
Dolerite Dyke
g
N
Altered Dolerite Dyke
h
N
Ultramafic Rocks
Dolerite Dyke

Figure 3.

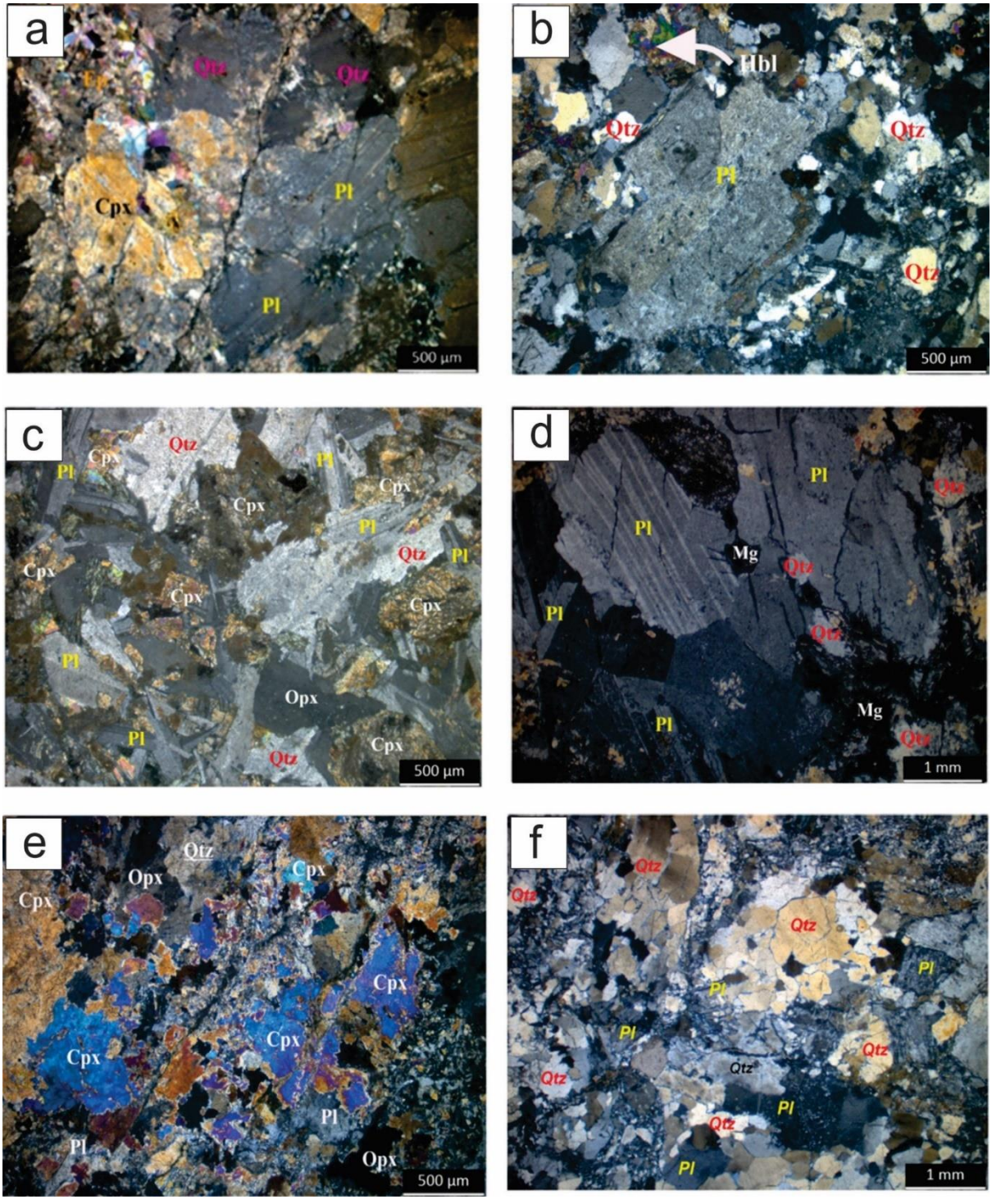

636

637 **Figure 4.**

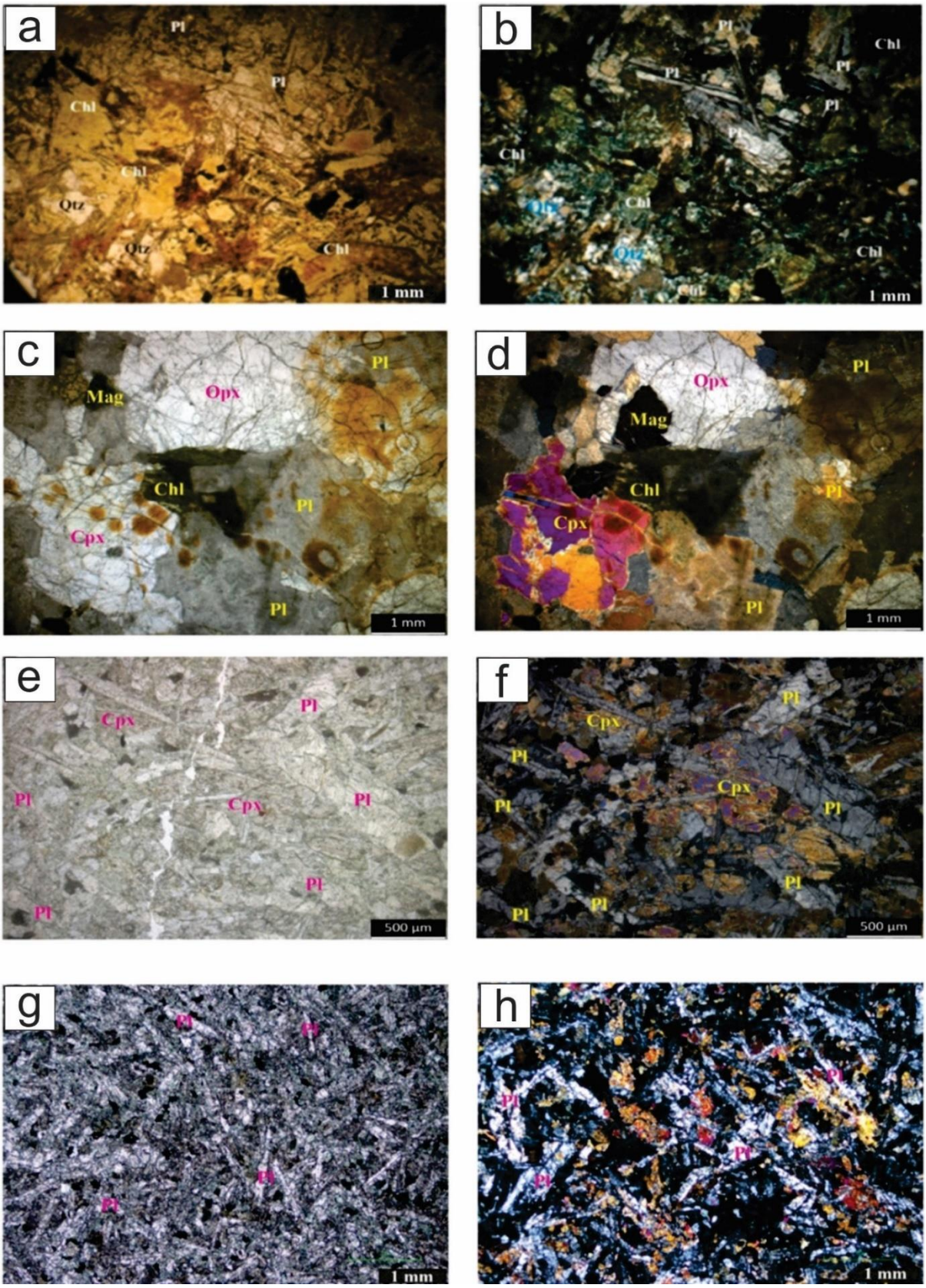

638

639 **Figure 5.**

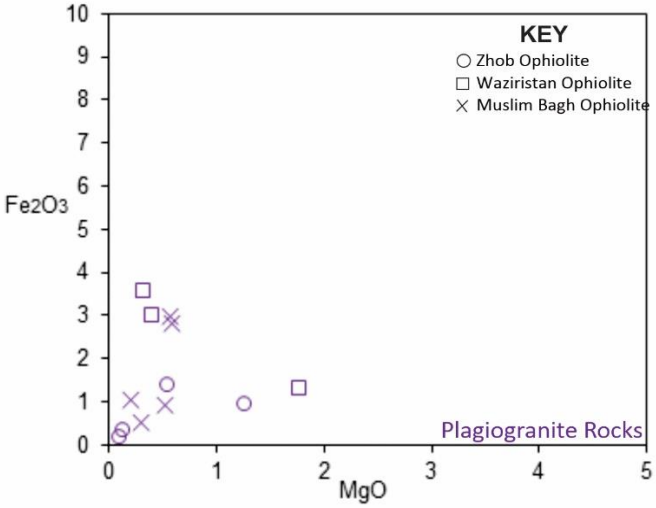
KEY
Zhob Ophiolite
Waziristan Ophiolite
Muslim Bagh Ophiolite
Fe2O3
MgO
Plagiogranite Rocks

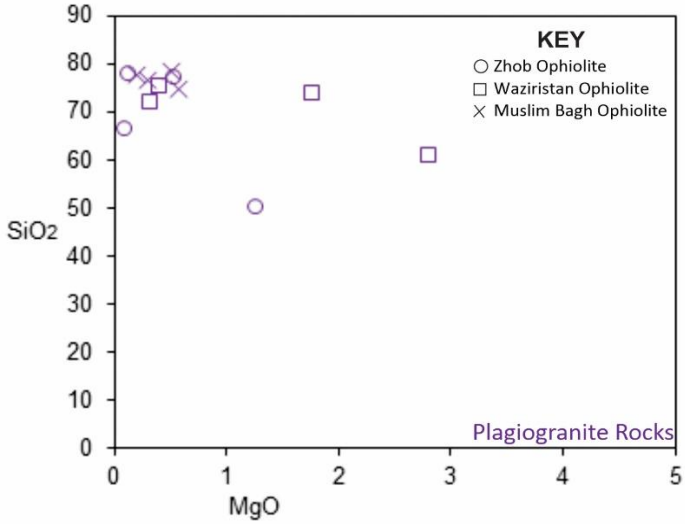
KEY
Zhob Ophiolite
Waziristan Ophiolite
Muslim Bagh Ophiolite
SiO2
MgO
Plagiogranite Rocks

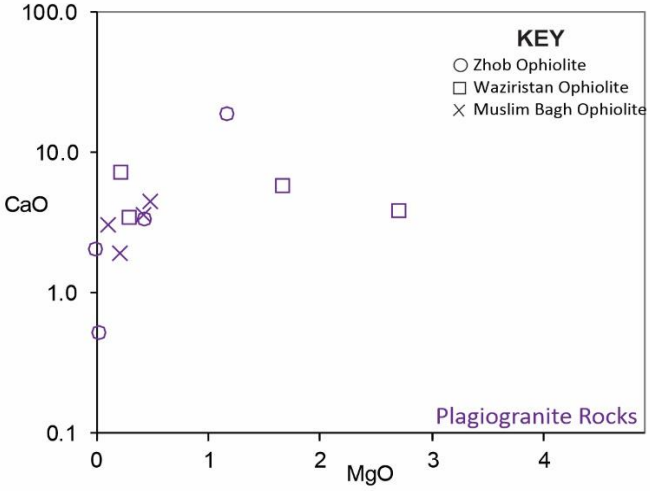
KEY
Zhob Ophiolite
Waziristan Ophiolite
Muslim Bagh Ophiolite
CaO
MgO
Plagiogranite Rocks

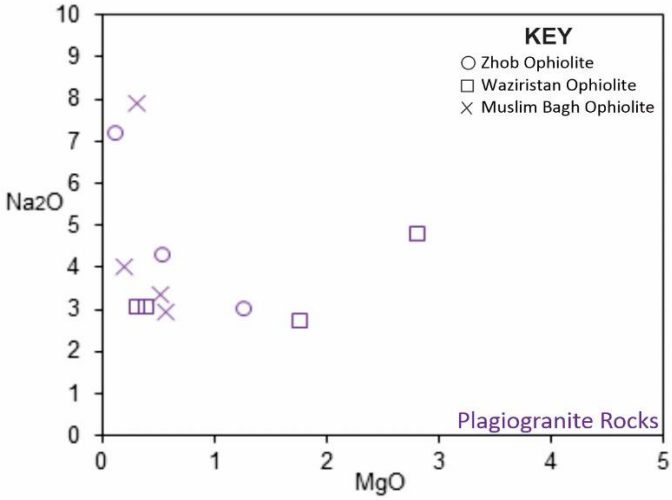
KEY
Zhob Ophiolite
Waziristan Ophiolite
Muslim Bagh Ophiolite
Na2O
MgO
Plagiogranite Rocks

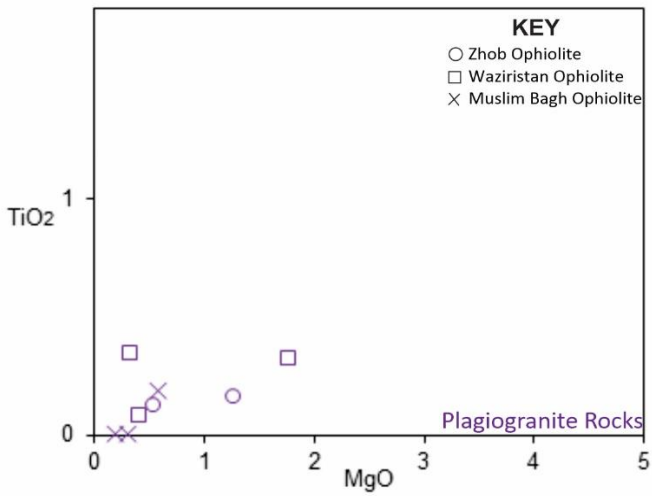
KEY
Zhob Ophiolite
Waziristan Ophiolite
Muslim Bagh Ophiolite
TiO2
MgO
Plagiogranite Rocks

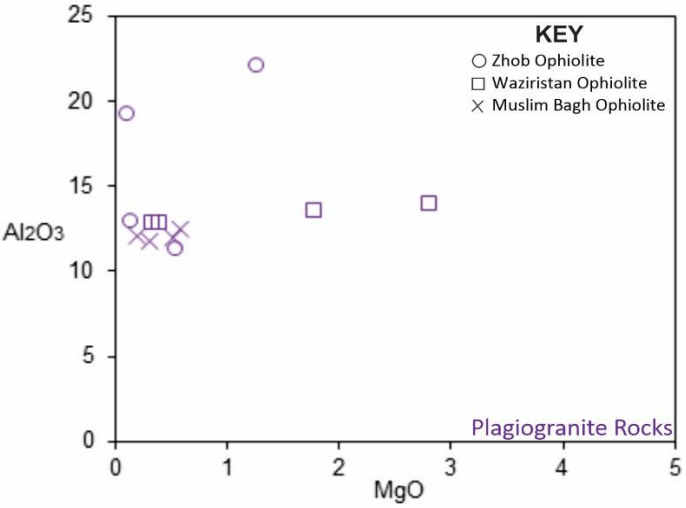
KEY
Zhob Ophiolite
Waziristan Ophiolite
Muslim Bagh Ophiolite
Al2O3
MgO
Plagiogranite Rocks

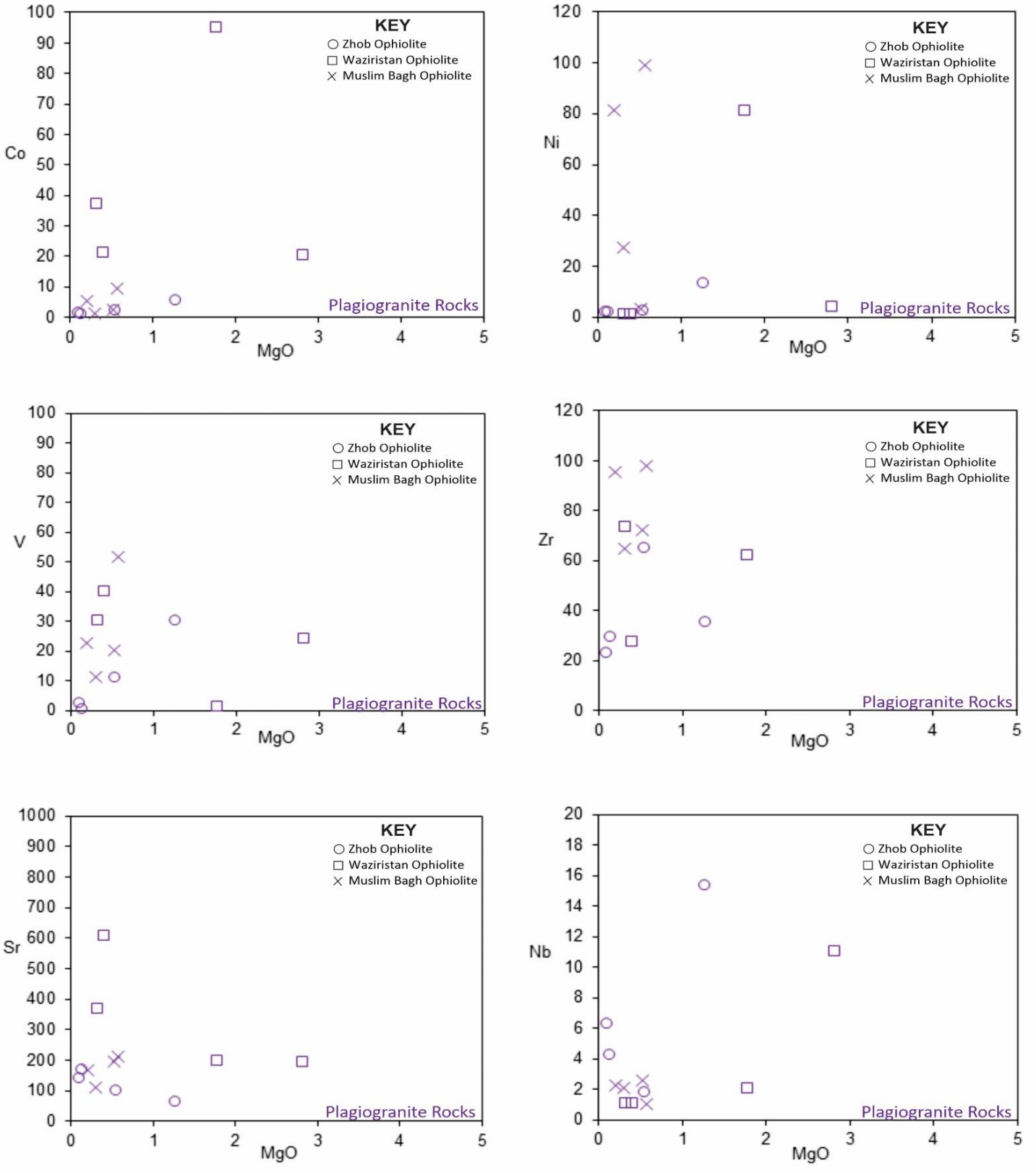

642 **Figure 6a.**

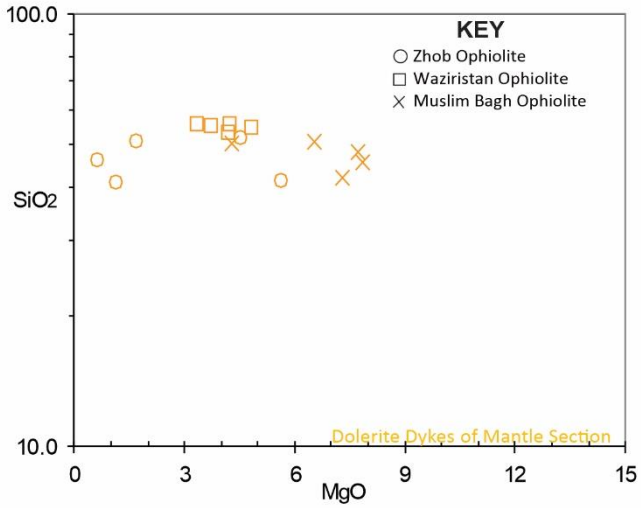
KEY
Zhob Ophiolite
Waziristan Ophiolite
Muslim Bagh Ophiolite
SiO2
MgO
Dolerite Dykes of Mantle Section

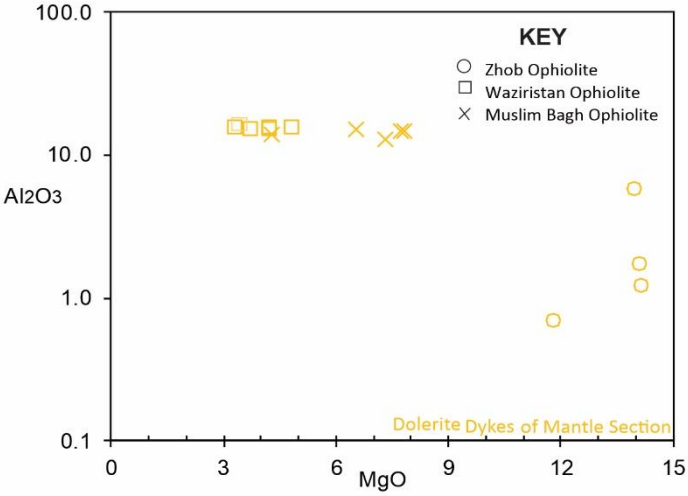
KEY
Zhob Ophiolite
Waziristan Ophiolite
Muslim Bagh Ophiolite
Al2O3
MgO
Dolerite Dykes of Mantle Section

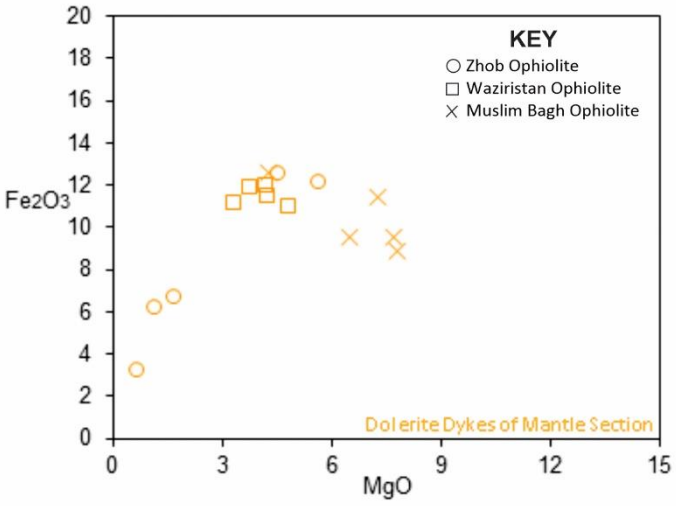
KEY
Zhob Ophiolite
Waziristan Ophiolite
Muslim Bagh Ophiolite
Fe2O3
MgO
Dolerite Dykes of Mantle Section

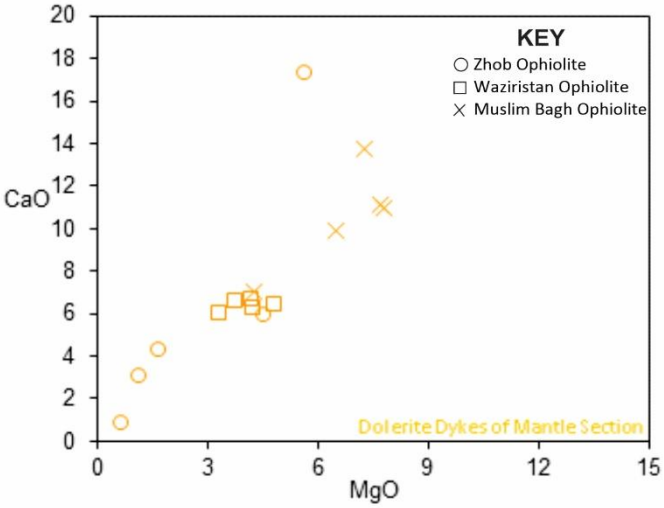
KEY
Zhob Ophiolite
Waziristan Ophiolite
Muslim Bagh Ophiolite
CaO
MgO
Dolerite Dykes of Mantle Section

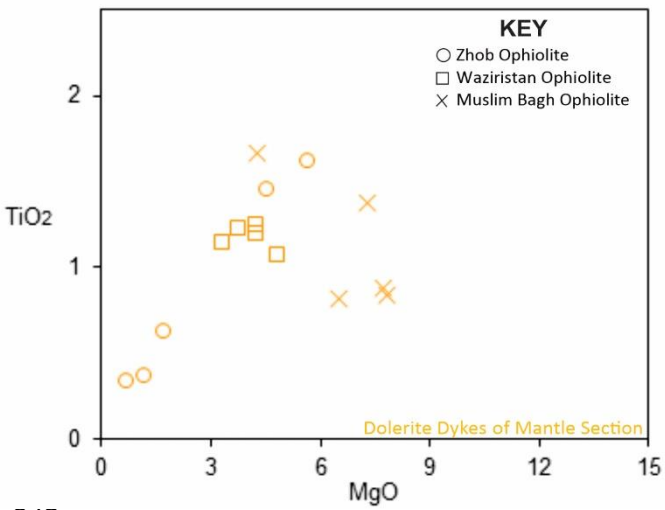
KEY
Zhob Ophiolite
Waziristan Ophiolite
Muslim Bagh Ophiolite
TiO2
MgO
Dolerite Dykes of Mantle Section

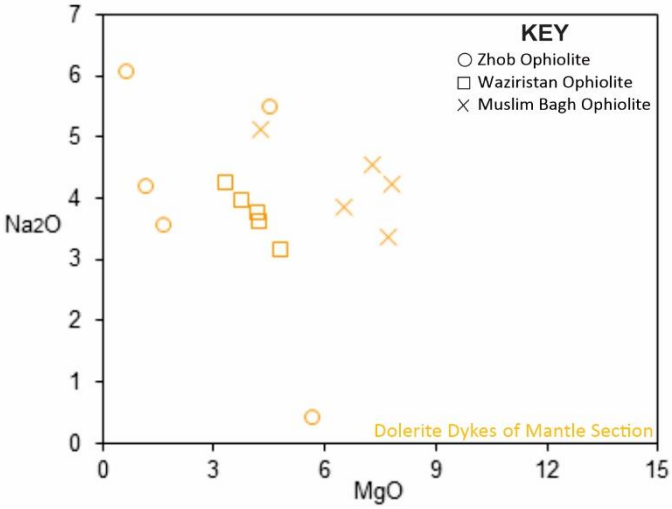
KEY
Zhob Ophiolite
Waziristan Ophiolite
Muslim Bagh Ophiolite
Na2O
MgO
Dolerite Dykes of Mantle Section

644

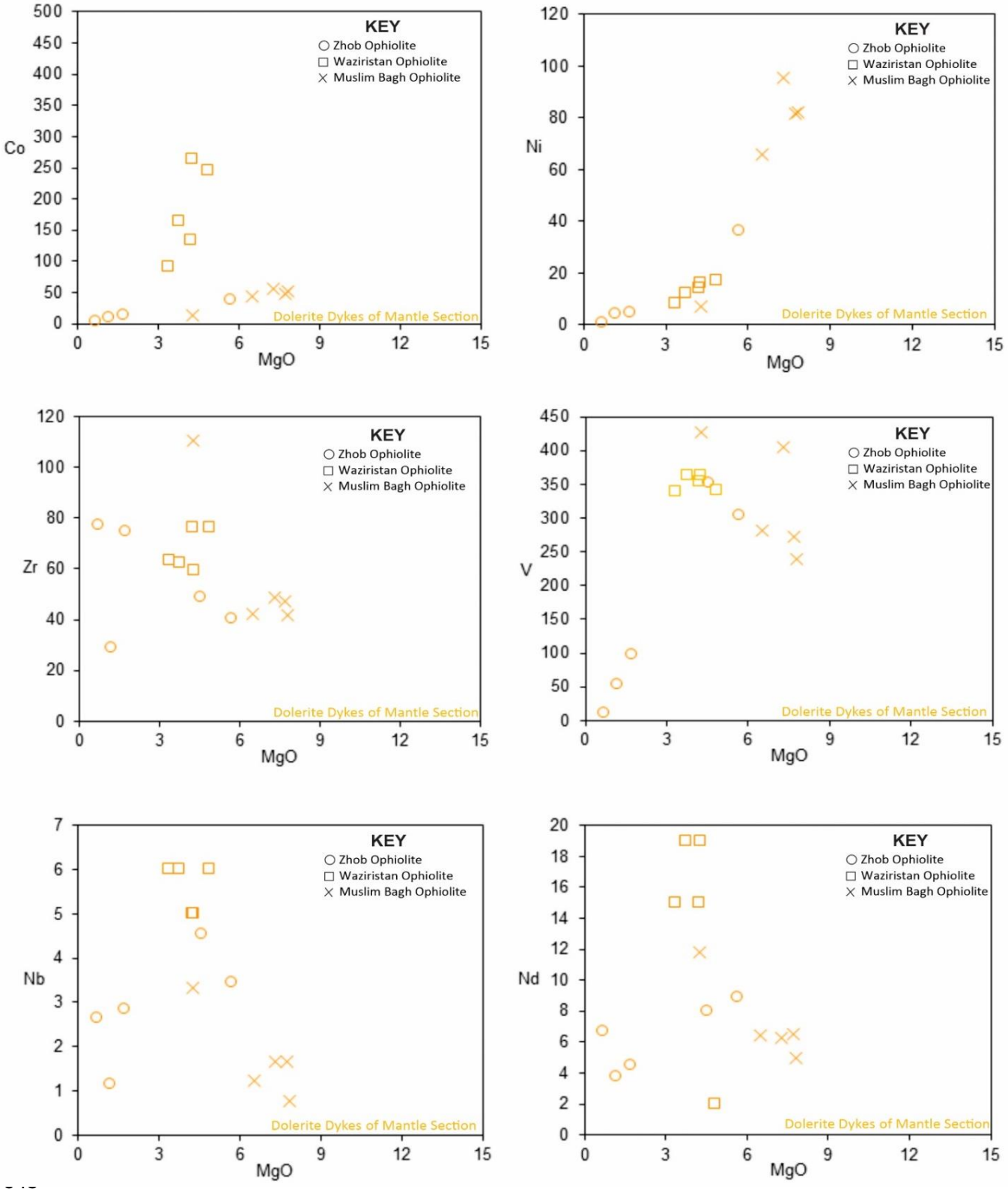
KEY
Zhob Ophiolite
Waziristan Ophiolite
Muslim Bagh Ophiolite
Dolerite Dykes of Mantle Section
Co
Ni
Zr
V
Nb
Nd
MgO

Figure 6b.

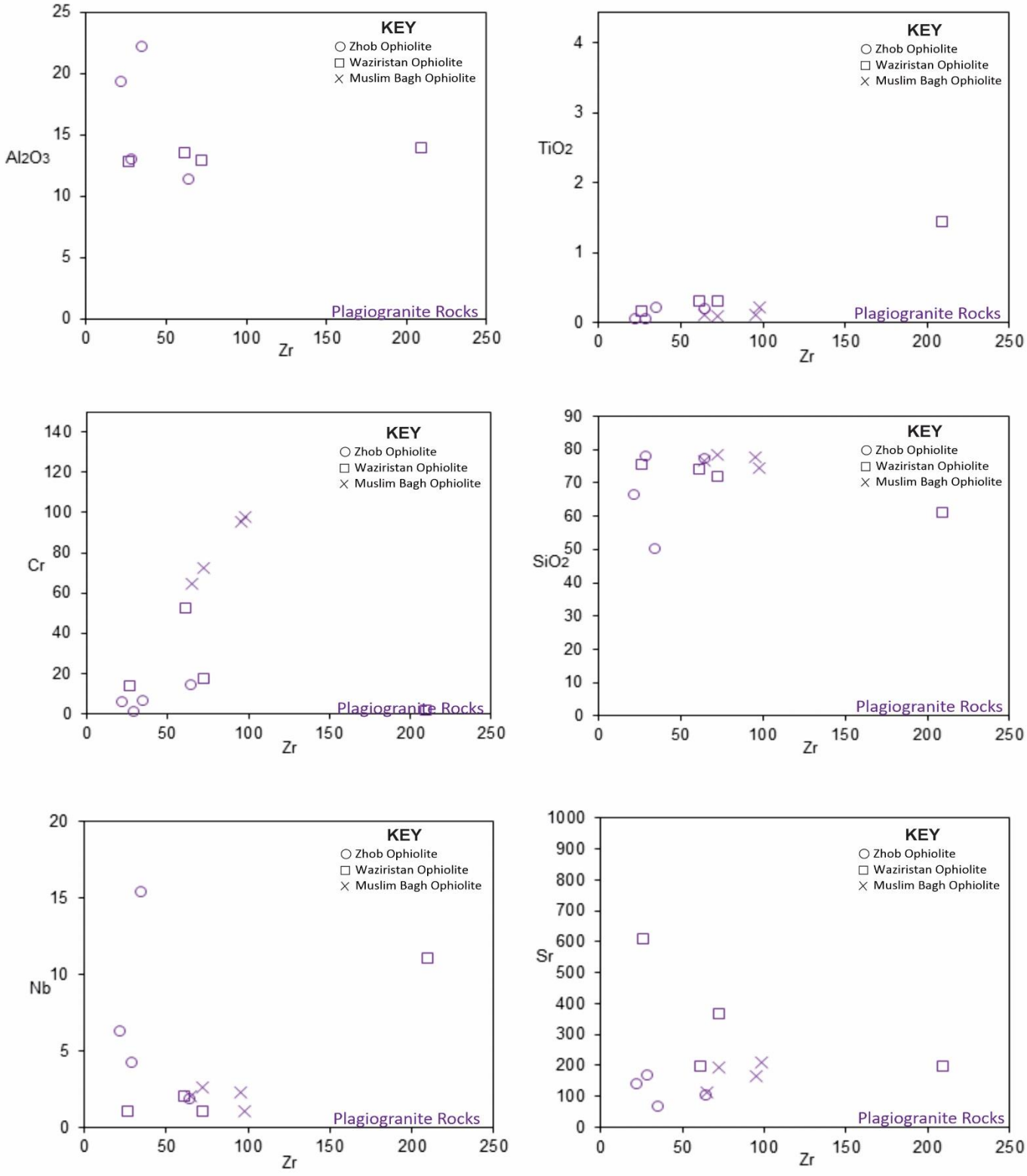
KEY
Zhob Ophiolite
Waziristan Ophiolite
Muslim Bagh Ophiolite
Plagiogranite Rocks
Al2O3
TiO2
Cr
SiO2
Nb
Sr
Zr

Figure 7a.

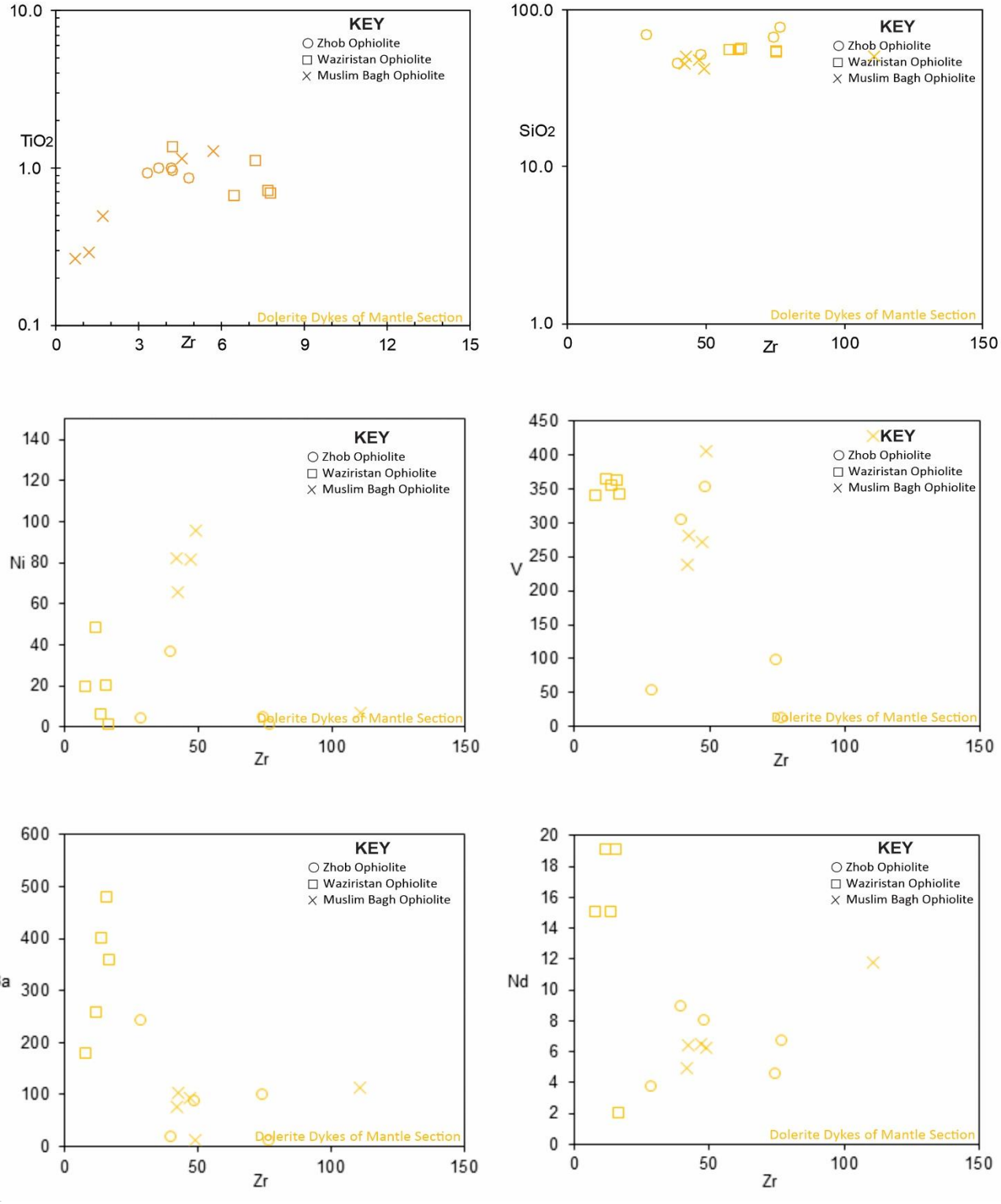

651 **Figure 7b.**

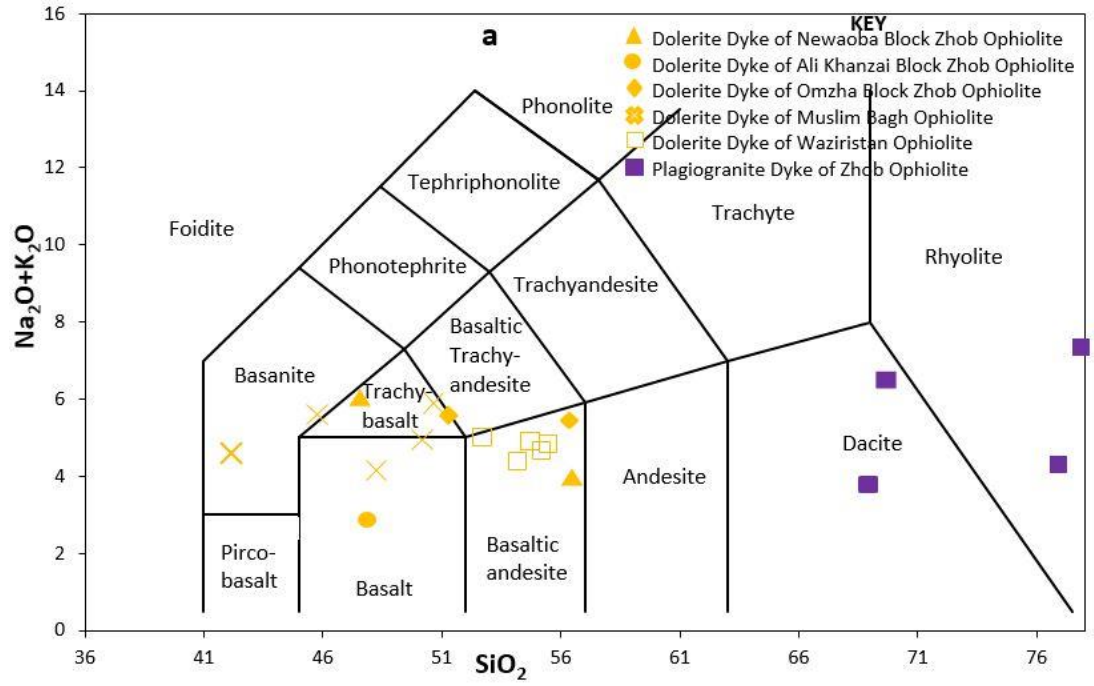

652

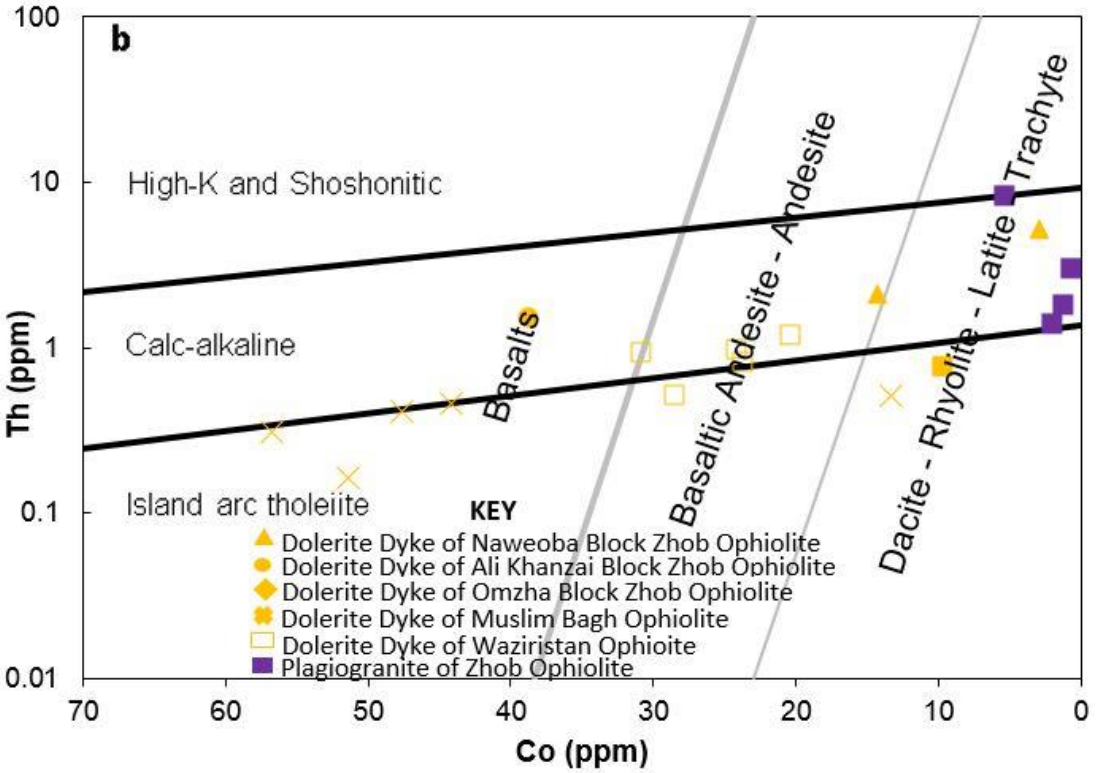

653

654

655 **Figure 8.**

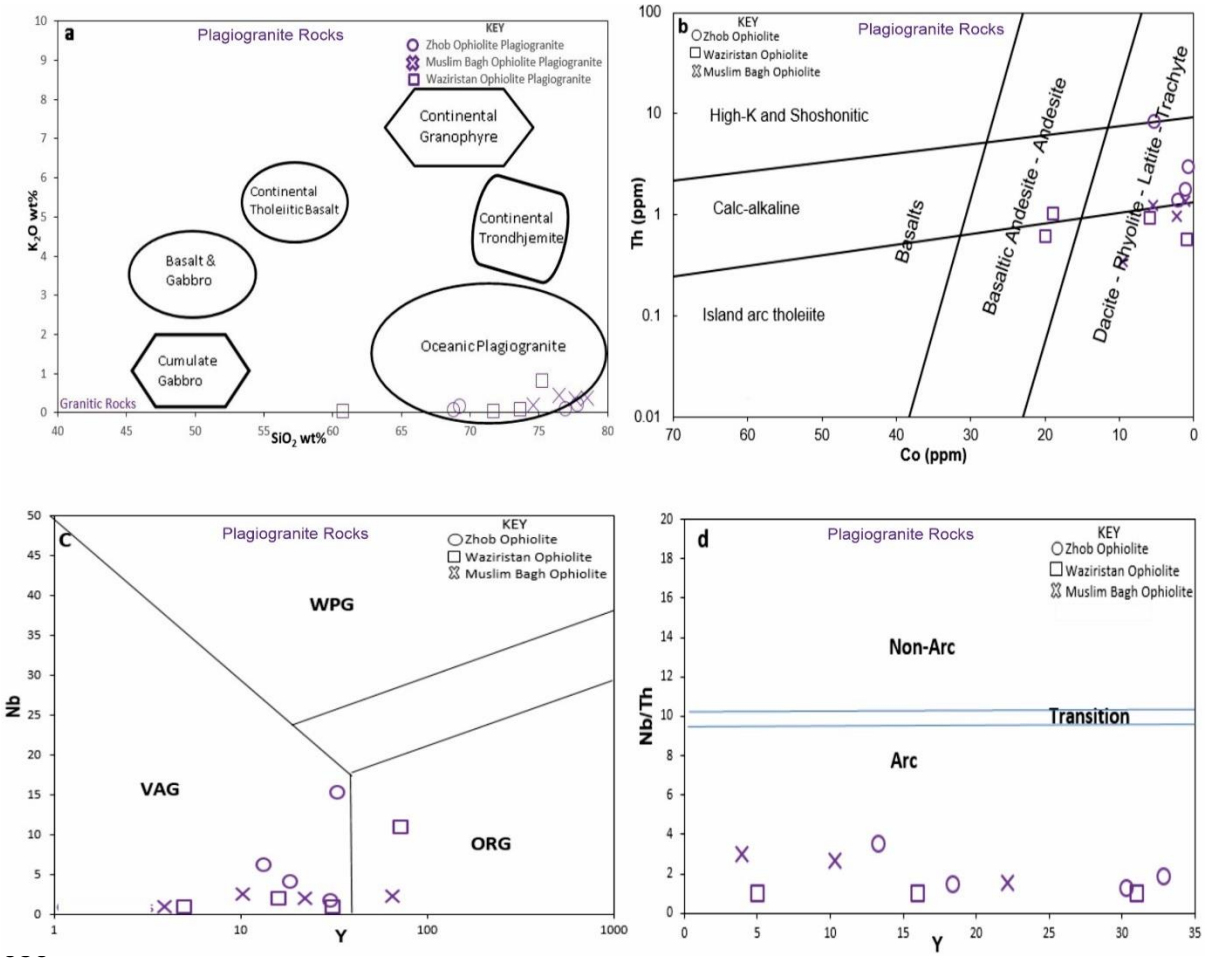

657 **Figure 9.**

658

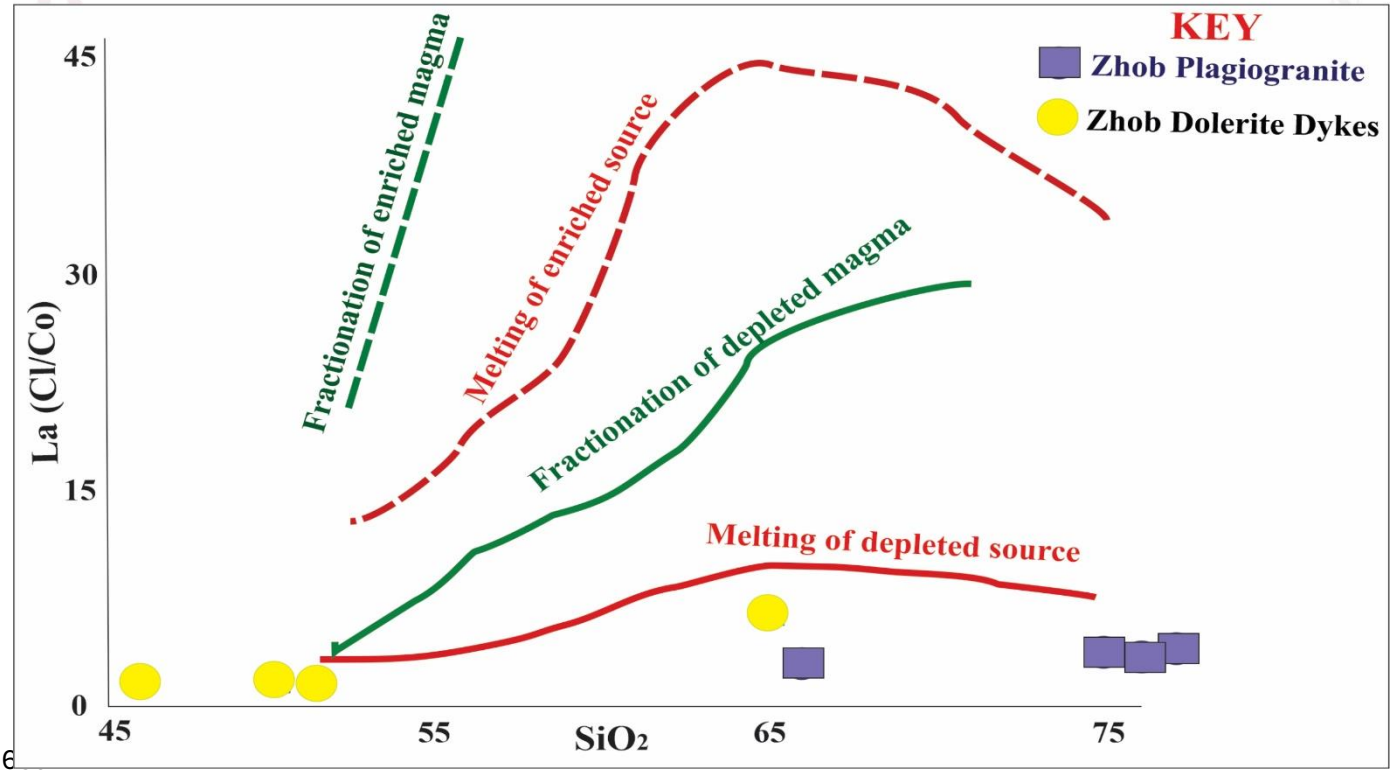

660

661 **Figure 10.**

662

663

664

665

666

667

668

669

670

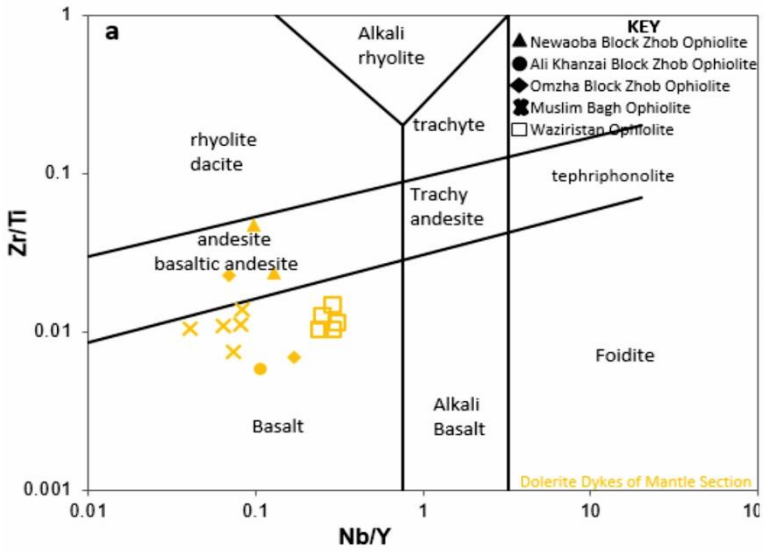
a
Alkali rhyolite
rhyolite dacite
trachyte
Trachy andesite
tephriphonolite
andesite basaltic andesite
Foidite
Basalt
Alkali Basalt
KEY
Newaoba Block Zhob Ophiolite
Ali Khanzai Block Zhob Ophiolite
Omzha Block Zhob Ophiolite
Muslim Bagh Ophiolite
Waziristan Ophiolite
Dolerite Dykes of Mantle Section
Zr/Ti
Nb/Y

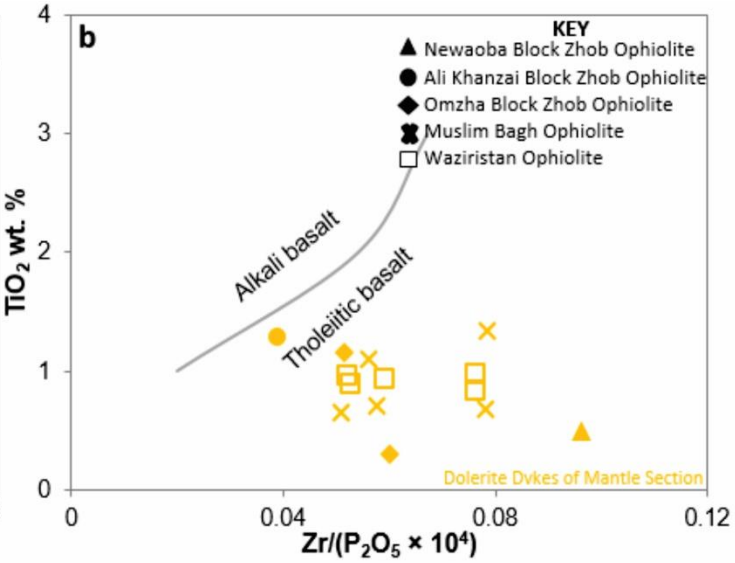
b
KEY
Newaoba Block Zhob Ophiolite
Ali Khanzai Block Zhob Ophiolite
Omzha Block Zhob Ophiolite
Muslim Bagh Ophiolite
Waziristan Ophiolite
Alkali basalt
Tholeiitic basalt
Dolerite Dykes of Mantle Section
TiO2 wt. %
Zr/(P2O5 × 10⁴)

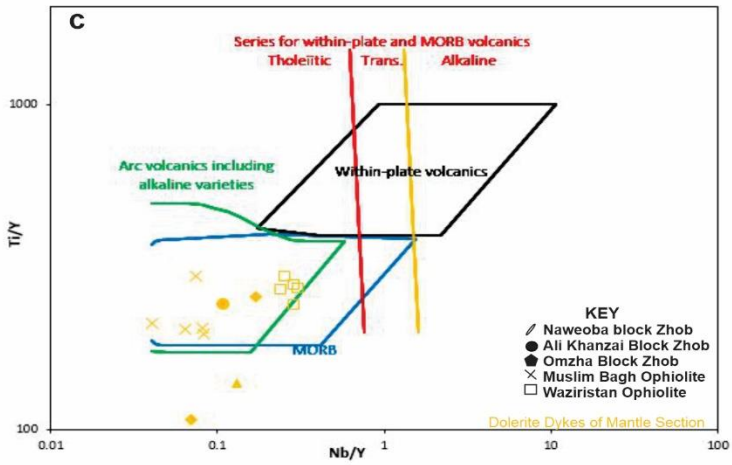
c
Series for within-plate and MORB volcanics
Tholeiitic
Trans.
Alkaline
Arc volcanics including alkaline varieties
Within-plate volcanics
MORB
KEY
Naweoba block Zhob
Ali Khanzai Block Zhob
Omzha Block Zhob
Muslim Bagh Ophiolite
Waziristan Ophiolite
Dolerite Dykes of Mantle Section
Ti/Y
Nb/Y

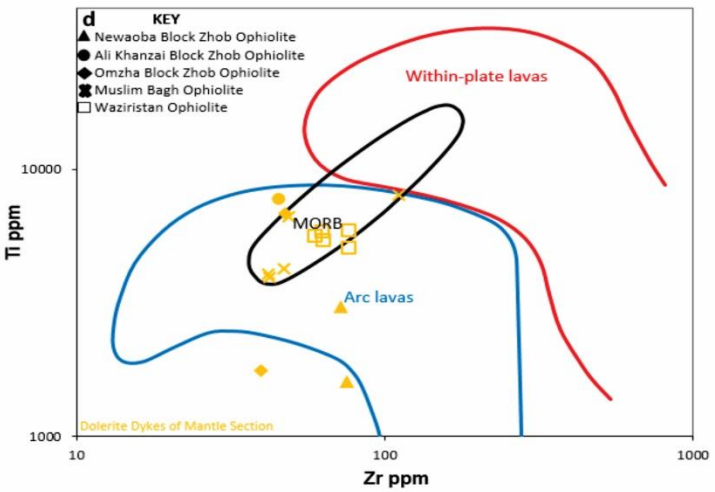
d
KEY
Newaoba Block Zhob Ophiolite
Ali Khanzai Block Zhob Ophiolite
Omzha Block Zhob Ophiolite
Muslim Bagh Ophiolite
Waziristan Ophiolite
Within-plate lavas
MORB
Arc lavas
Dolerite Dykes of Mantle Section
Ti ppm
Zr ppm

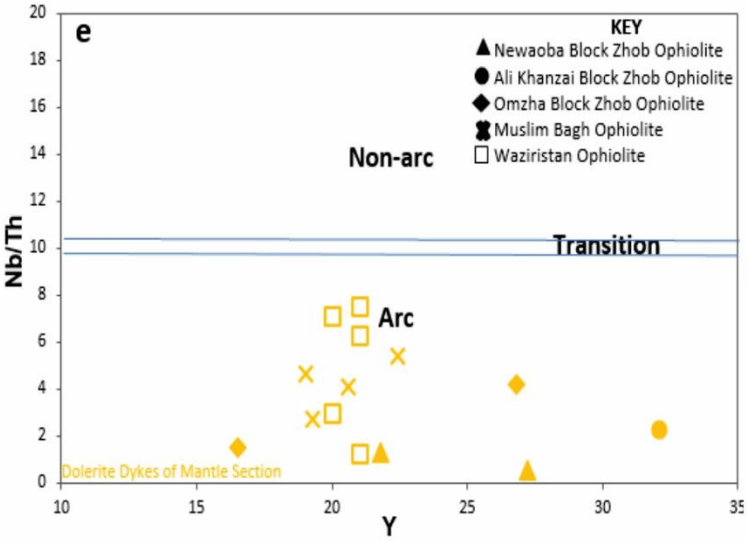
e
KEY
Newaoba Block Zhob Ophiolite
Ali Khanzai Block Zhob Ophiolite
Omzha Block Zhob Ophiolite
Muslim Bagh Ophiolite
Waziristan Ophiolite
Non-arc
Transition
Arc
Dolerite Dykes of Mantle Section
Nb/Th
Y

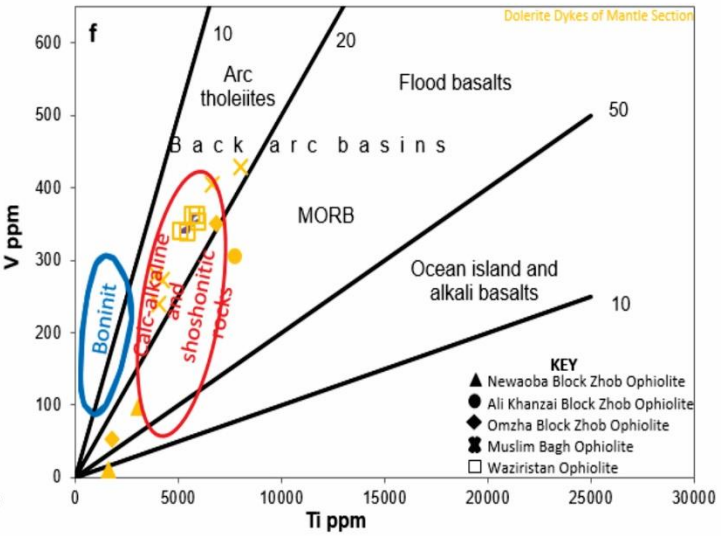
f
Dolerite Dykes of Mantle Section
10
20
50
Arc tholeiites
Flood basalts
Back arc basins
MORB
Ocean island and alkali basalts
Boninit
Calc-alkaline and shoshonitic rocks
KEY
Newaoba Block Zhob Ophiolite
Ali Khanzai Block Zhob Ophiolite
Omzha Block Zhob Ophiolite
Muslim Bagh Ophiolite
Waziristan Ophiolite
V ppm
Ti ppm

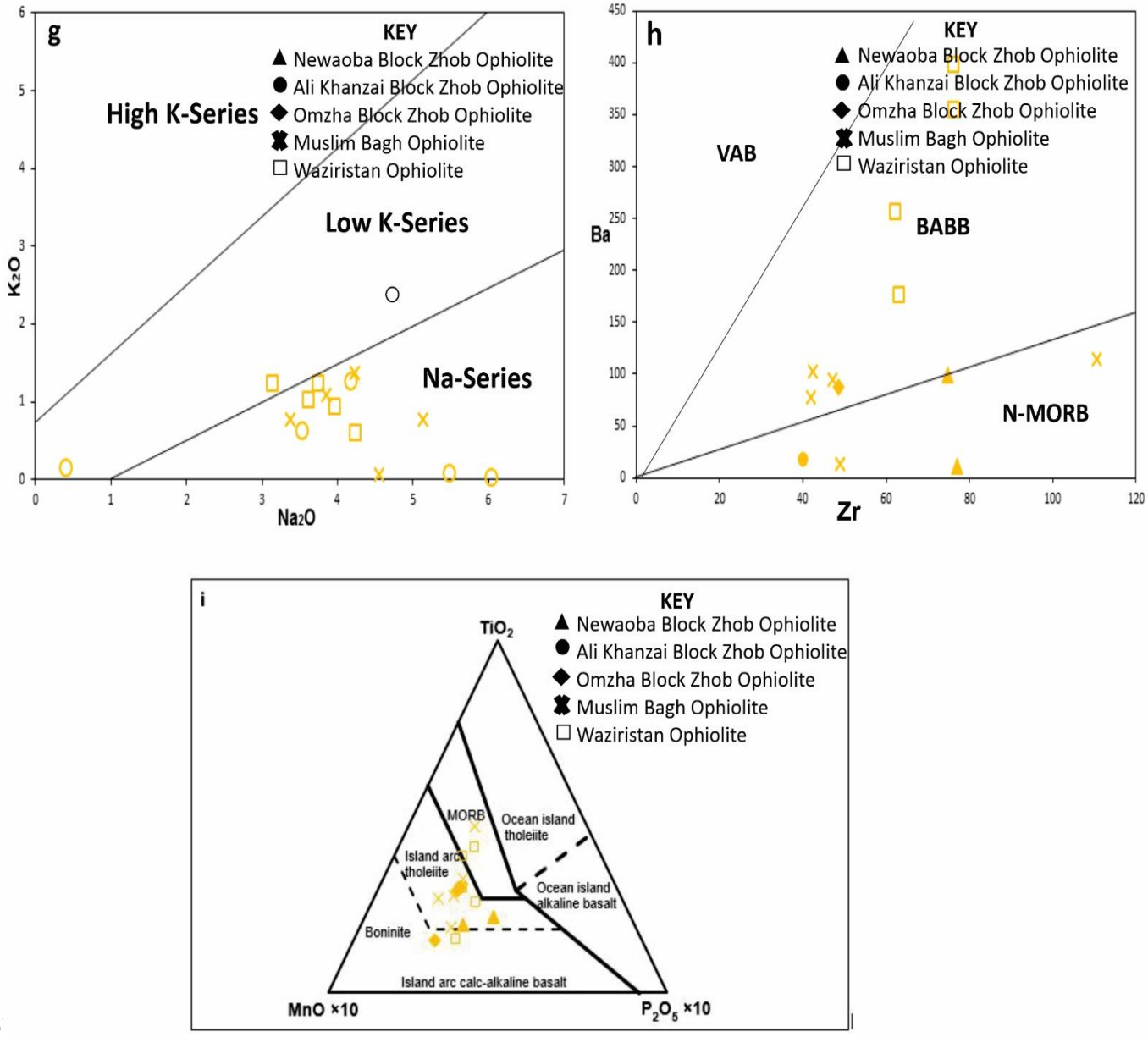
g
KEY
Newaoba Block Zhob Ophiolite
Ali Khanzai Block Zhob Ophiolite
Omzha Block Zhob Ophiolite
Muslim Bagh Ophiolite
Waziristan Ophiolite
High K-Series
Low K-Series
Na-Series
K2O
Na2O
h
KEY
Newaoba Block Zhob Ophiolite
Ali Khanzai Block Zhob Ophiolite
Omzha Block Zhob Ophiolite
Muslim Bagh Ophiolite
Waziristan Ophiolite
VAB
BABB
N-MORB
Ba
Zr
i
KEY
Newaoba Block Zhob Ophiolite
Ali Khanzai Block Zhob Ophiolite
Omzha Block Zhob Ophiolite
Muslim Bagh Ophiolite
Waziristan Ophiolite
TiO2
MORB
Ocean island tholeiite
Island arc tholeiite
Ocean island alkaline basalt
Boninite
Island arc calc-alkaline basalt
MnO ×10
P2O5 ×10

Figure 11.

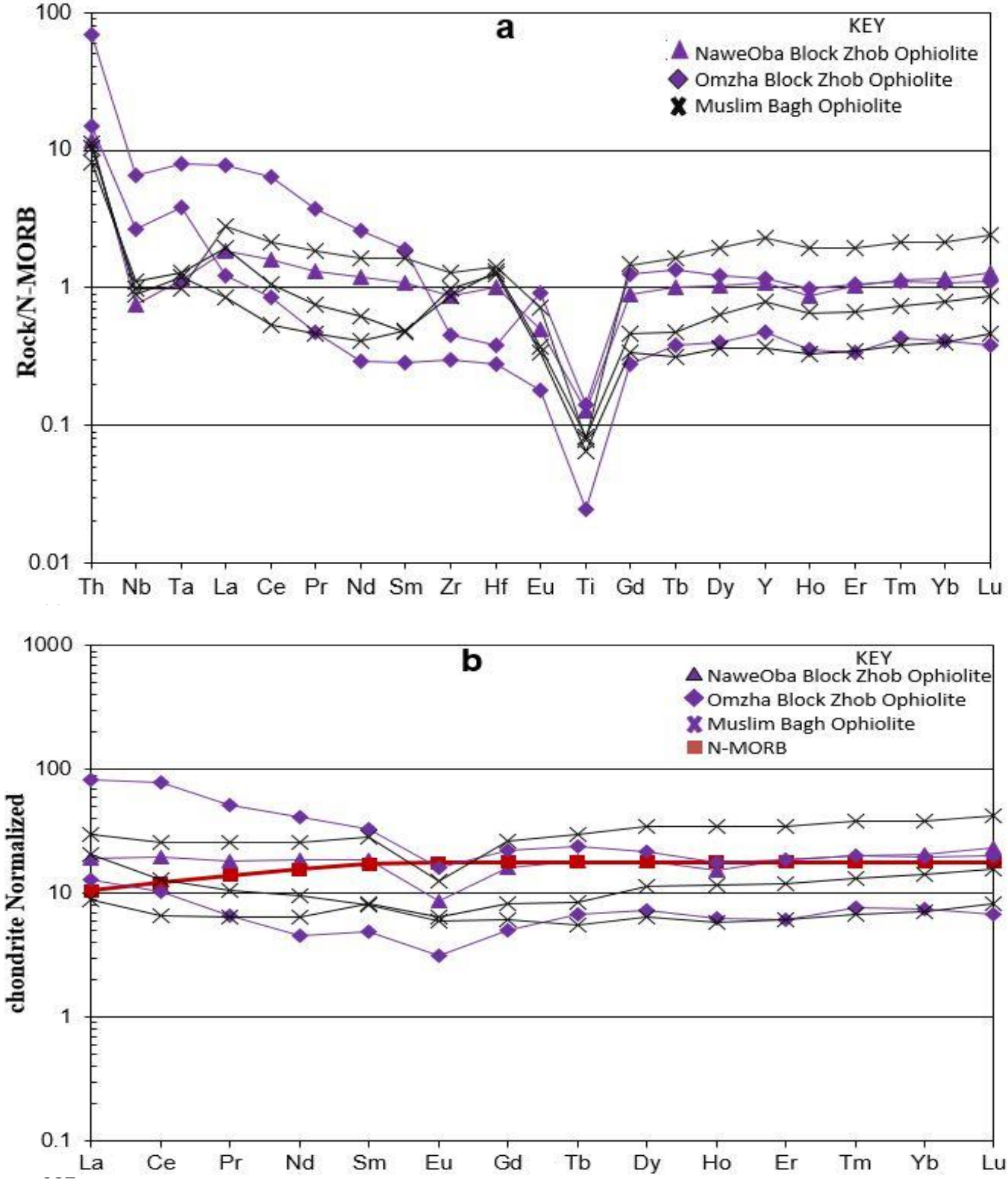

683 **Figure 12.**

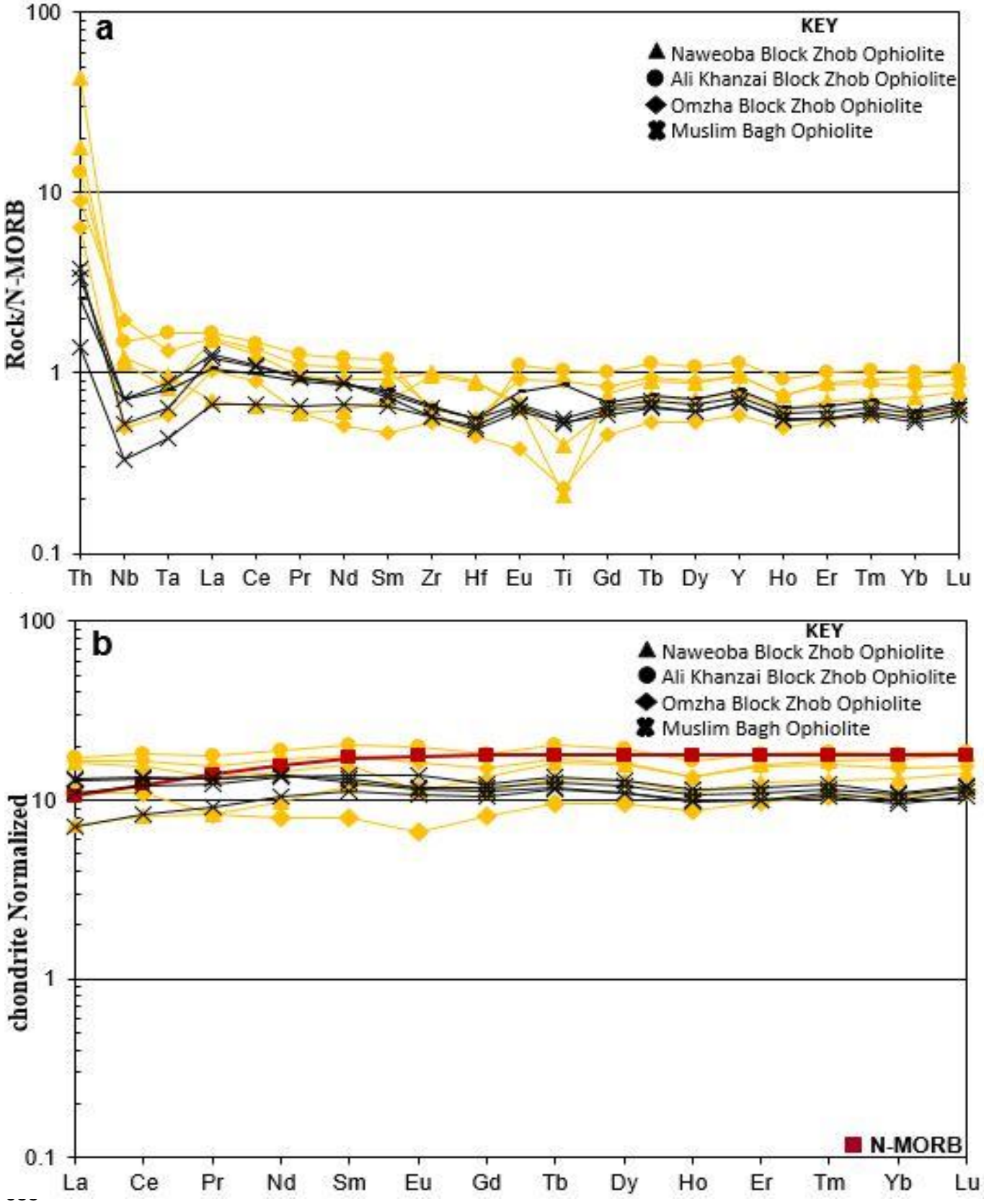
a
KEY
Naweoba Block Zhob Ophiolite
Ali Khanzai Block Zhob Ophiolite
Omzha Block Zhob Ophiolite
Muslim Bagh Ophiolite
Rock/N-MORB
100
10
1
0.1
Th Nb Ta La Ce Pr Nd Sm Zr Hf Eu Ti Gd Tb Dy Y Ho Er Tm Yb Lu
b
KEY
Naweoba Block Zhob Ophiolite
Ali Khanzai Block Zhob Ophiolite
Omzha Block Zhob Ophiolite
Muslim Bagh Ophiolite
chondrite Normalized
100
10
1
0.1
N-MORB
La Ce Pr Nd Sm Eu Gd Tb Dy Ho Er Tm Yb Lu

Figure 13.

688 **Table 1**. Major oxides (wt %), trace and REE elements (ppm) of the doleritic and
689 plagiogranite dykes of the Zhob ophiolite.
690

Sample No	NB 08	NB 20	AK 30	OMZ 03	OMZ 04	NB 45	OMZ 06	OMZ 43	OMZ 49
Rock Type	Dolerite	Dolerite	Dolerite	Dolerite	Dolerite	Plagiogranite	Plagiogranite	Plagiogranite	Plagiogranite
SiO_2	56.69	47.61	47.93	51.31	56.70	76.94	69.29	77.85	68.85
TiO_2	0.50	0.27	1.29	1.16	0.29	0.16	0.03	0.04	0.18
Al_2O_3	14.12	12.84	13.99	15.20	14.20	11.29	18.23	12.92	10.07
Fe_2O_3	10.68	11.19	12.06	12.47	11.12	1.35	0.16	0.31	0.92
MnO	0.13	0.05	0.20	0.19	0.12	0.02	0.01	0.01	0.02
MgO	1.71	4.68	5.68	4.56	1.19	0.55	0.11	0.14	1.28
CaO	4.22	9.79	14.28	5.92	3.99	3.26	2.01	0.51	11.41
Na_2O	3.53	6.04	0.41	5.48	4.18	4.25	10.42	7.15	2.99
K_2O	0.62	0.02	0.16	0.08	1.27	0.07	0.14	0.19	0.05
P_2O_5	0.08	0.05	0.10	0.09	0.05	0.02	0.05	0.06	0.12
Cr_2O_3	0.00	0.00	0.01	0.00	0.00	0.00	0.00	0.00	0.00
LOI	6.55	6.09	2.72	1.86	6.20	0.13	0.40	0.26	4.19
Total	**98.92**	**98.61**	**98.84**	**98.33**	**99.31**	**98.04**	**98.84**	**99.45**	**100.08**
Sc	20.5	8.1	42.9	31.1	19.6	8.7	3.0	1.2	21.4
V	97.0	11.0	303.9	351.4	52.4	11.1	2.4	0.3	30.2
Cr	6.5	4.5	39.1	8.4	2.8	13.9	5.5	0.7	6.1
Co	14.3	2.9	38.7	552.0	9.7	2.1	1.2	0.8	5.3
Ni	4.4	0.6	36.3	500.7	3.9	2.4	1.8	1.9	13.2
Cu	16.0	40.2	97.1	173.3	8.1	3.2	1.9	1.8	4.4
Zn	58.2	14.7	66.8	69.1	55.2	8.7	2.1	26.3	8.9
Sr	135.2	68.2	134.9	799.9	614.3	96.15	131.85	163.65	59.6
Y	20.8	26.8	31.4	26.1	16.35	30.00	13.1	18.9	32.25
Zr	74.7	77.0	40.0	48.7	29.0	64.9	22.6	29.3	35.4
Ba	99.05	11.85	18.4	86.45	238.9	12.35	43.75	39.6	8.75
Ga	11.6	9.5	12.6	13.6	10.9	10.8	6.5	8.5	16.0
Rb	5.6	0.7	1.3	1.4	13.9	0.9	1.6	2.3	1.1
Nb	2.83	2.65	3.45	4.54	1.16	1.77	6.26	4.23	15.35
Cs	0.03	0.01	0.04	0.02	0.55	0.02	0.02	0.03	0.01
La	1.74	3.82	4.14	3.88	2.59	4.58	3.04	5.03	19.37
Ce	4.94	9.54	11.04	10.10	6.79	12.11	6.39	13.27	48.24
Pr	0.80	1.28	1.68	1.45	0.79	1.74	0.63	1.43	4.89
Nd	4.52	6.69	8.86	7.95	3.73	8.78	2.12	5.43	19.20
Sm	1.84	2.40	3.09	2.74	1.21	2.87	0.75	1.48	5.02
Eu	0.70	0.66	1.14	0.94	0.39	0.51	0.18	0.02	0.94
Gd	2.29	2.80	3.76	3.09	1.67	3.32	1.04	1.62	4.56
Tb	0.49	0.60	0.76	0.64	0.35	0.67	0.25	0.35	0.89
Dy	3.24	4.02	4.96	4.11	2.44	4.66	1.83	2.44	5.55
Ho	0.62	0.76	0.94	0.77	0.50	0.88	0.36	0.49	1.00
Er	2.07	2.61	3.00	2.54	1.63	3.07	1.01	1.66	3.11
Tm	0.33	0.42	0.47	0.40	0.27	0.51	0.20	0.32	0.51
Yb	2.25	2.85	3.06	2.57	1.78	3.53	1.26	2.22	3.31
Lu	0.36	0.46	0.47	0.39	0.28	0.59	0.17	0.37	0.51

Hf	1.80	1.86	0.94	1.14	0.91	2.06	0.57	1.13	0.78
Ta	0.13	0.11	0.22	0.18	0.08	0.15	0.51	0.39	1.06
Pb	2.59	2.25	1.73	1.27	3.01	1.20	0.27	2.58	13.46
Th	2.16	5.19	1.54	1.08	0.77	1.40	1.80	3.00	8.36
U	0.17	0.43	0.20	0.25	0.16	0.55	0.72	0.73	1.98